HYF-12

THE UNIVERSITY OF MICHIGAN

College of Engineering
Department of Naval Architecture and Marine Engineering

COLLISION PROTECTION OF NUCLEAR SHIPS

A Survey of the State of the Art

Odo Krappinger

ORA Project No. 07990

under contract with:

Maritime Administration
U. S. Department of Commerce
Contract No. MA-2564
Task No. 9

Administered through:

May 1966

OFFICE OF RESEARCH ADMINISTRATION · ANN ARBOR

THE UNIVERSITY OF MICHIGAN

College of Engineering
Department of Naval Architecture and Marine Engineering

COLLISION PROTECTION OF NUCLEAR SHIPS

A Survey of the State of the Art

Odo Krappinger

ORA Project No. 07990

under contract with:

Maritime Administration
U. S. Department of Commerce
Contract No. MA-2564
Task No. 9

Administered through:
Office of Research Administration

May 1966
Ann Arbor

ACKNOWLEDGMENTS

I am most grateful to Professor Ernest Frankel, who has initiated this study and has helped to provide me with literature. I also want to thank Präsident Böhnecke, Dr. Drittler, Dipl. Ing. Riepe and Dipl. Ing. Seefisch, all of Hamburg, Professor Spinelli of Naples and Mr. Woisin of Hamburg for their quick response when I asked them for recent literature on collision protection of nuclear ships.

I am indebted to the staff of the Department of Naval Architecture and Marine Engineering of The University of Michigan. Whenever necessary all of them have lent me a helpful hand. My sincere thanks go to Professor Harry Benford, who read the manuscript in order to improve the language.

CONTENTS

SUMMARY

A survey of the literature shows that since the design of N. S. SAVANNAH the progress of research made in the field of collision protection of nuclear power plants has been only modest. It seems that it has not been recognized that basic research is necessary in order to find satisfactory solutions for this problem. Therefore many questions cannot as yet be answered.

This study tries to show how the whole problem of collision protection can be broken down. It also summarizes the state of the art with regard to the individual aspects of the problem. It is hoped, that the study will be of some help in finding starting points for a more organized and systematic approach in the future.

INTRODUCTION

The design of the collision protection for the reactor of the SAVANNAH is an admirable piece of engineering. Because sufficient scientific background for this task was lacking, the designers had to use ingenuity and intuition to find a solution. Such an approach is not unusual; there are many examples in the field of engineering, where the creation of a feasible solution preceded the complete understanding of the problem. Though this is good enough for the first realization of an idea, or for a single object, it is not sufficient for the future development. The desire for progress and the necessity for judging new and competing ideas require a broader and more thorough understanding of the fundamentals. In our case this means that some basic research has to be done -- not with regard to an individual ship but with the goal of the general understanding and quantitative description of all the phenomena of ship collision. For this purpose it is necessary to break the whole problem down into manageable portions. Such a classification is also useful for the review and analysis of the literature in collision protection that is made in this study.

The following breakdown will be used:

1. External mechanics of impact
2. Internal mechanics of impact (behavior of structures)
3. Stochastic aspect of collisions
4. Ideas and suggestions for protection structures

Item 1 is essentially the classical approach in dealing with impacts and is therefore a good starting point. Under this heading I will discuss also some peculiarities of ship collisions. Item 2 covers the problem of energy absorbtion of ship structures. Item 3 deals with the environmental factors of collisions (e.g., speed, size of potential collision partner, etc.). Because these are not known for certain, stochastic methods have to be used. The last item reports some creative ideas rather than the results of systematic investigations.

1. EXTERNAL MECHANICS OF IMPACT

1.1 General

With regard to the struck vessel we can differentiate between four different kinds of impact:

1. Direct central impact, see the example in Figure 1.

2. Direct eccentric impact, see the example in Figure 2.

3. Oblique central impact, see the examples in Figure 3.

4. Oblique eccentric impact, see the examples in Figure 4.

Cases 1 and 2 are relatively simple. The energy transformed into plastic deformation and destruction of material is

$$\Delta E = \tfrac{1}{2} V_A^2 m_A (1-e^2) \frac{m_B}{m_A + m_B} \qquad \text{for case 1}$$

$$\Delta E = \tfrac{1}{2} V_A^2 m_A (1-e^2) \frac{m_B^*}{m_A + m_B^*} \qquad \text{for case 2}$$

$$\text{with} \quad m_B^* = \frac{i_B^2}{i_B^2 + p_B^2} m_B$$

where

V_A = speed of striking vessel

V_B = speed of struck vessel

m_A = mass plus added mass of vessel A

m_B = mass plus added mass of vessel B

m_B^* = reduced mass plus added mass of vessel B

i_B = radius of gyration (including added mass effects) of vessel B

p_B = perpendicular distance between the relevant speed and the center of gravity of vessel B (refer to the figures)

e = coefficient of restitution (e = 1 for perfectly elastic bodies; e = 0 for absolutely inelastic bodies)

In order to deal with the cases 3 and 4 we have to make some assumptions with regard to the acting impact forces. In most text books of engineering mechanics it is assumed that forces act only perpendicular to the plane of contact. It seems that this concept has been taken over by Minorsky (1959) and Castagneto (1962). (Figure 3a and 4a are based on this assumption.) Contrary to it, Woisin (1962) and (1964a), assumes that the forces act colinear with the relative speed between the two vessels (Figure 3b and 4b are based on this assumption.) There are also other assumptions that can be thought of.

Minorsky argues that we are primarily interested in penetrations normal to the struck ship's centerline. In doing so, he is however overlooking the fact that these penetrations certainly are not independent of the forces acting parallel to the centerline of the struck ship. Therefore, the approach suggested by Woisin seems to me more realistic. But it is also more complicated and it would be of practical use only if we also understand the behavior of the structure during oblique impact. Because this knowledge is still lacking I would suggest using the concept that the forces act only normal to the plane of contact (or practically to the centerline of the struck ship). When dealing with the behavior of the structures, this approximation should be kept in mind (see Chapter 2).

The energy transformed into plastic deformation and destruction of material for oblique impacts is:

for case 3a (shown in Figure 3a):

$$\Delta E = \tfrac{1}{2} V_{red}^2 \, m_A^* \, (1-e^2) \, \frac{m_B}{m_A^* + m_B}$$

for case 3b (shown in Figure 3b):

$$\Delta E = \tfrac{1}{2} V_{rel}^2 \, m_A^* \, (1-e^2) \, \frac{m_B}{m_A^* + m_B}$$

for case 4a (shown in Figure 4a):

$$\Delta E = \tfrac{1}{2} V_{red}^2 \, m_A^* \, (1-e^2) \, \frac{m_B^*}{m_A^* + m_B^*}$$

for case 4b (shown in Figure 4b):

$$\Delta E = \tfrac{1}{2}V_{rel}^2 \, m_A^* \, (1-e^2) \, \frac{m_B^*}{m_A^* + m_B^*}$$

with

$$m_A^* = \frac{i_A^2}{i_A^2 + p_A^2} \, m_A$$

$$m_B^* = \frac{i_B^2}{i_B^2 + p_B^2} \, m_B$$

where

V_{red} = speed component normal to plane of contact

V_{rel} = relative speed between vessels

m_A^* = reduced mass plus added mass of vessel A

i_A = radius of gyration (including added mass effects) of vessel A

p_A = perpendicular distance between the relevant speed vector and the center of gravity of vessel A

others same as above.

As can be seen from the foregoing, the general description of the mechanism of impact is relatively simple. But, there are some problems involved that are particular to ship collisions.

We will deal with some of them in the following chapters. Others are very complex and it is not likely that we will be able to take them into account in the foreseeable future. In reality the impact is not a two-dimensional problem as assumed above. The struck ship will not only turn around a vertical axis, it will in most cases also heel. Further, it seems possible that the bow of a striking ship with a raking stem can be lifted by the impact. It would be very troublesome to include all these effects.

1.2 Effects of the Surrounding Water

As has been shown in (Criteria)*, Section 4, Appendix 4A, the ship resistance that is proportional to the square of the speed is negligibly small. But there are also hydrodynamic forces, proportional to the accelerations, which are of big influence. The proportionality factors are variously known as entrained water, added mass or hydrodynamic mass.

In the SAVANNAH approach the added mass of the striking vessel was assumed to be zero. Forty percent of the actual mass of the struck vessel have been assumed as added mass. It also has been pointed out that a fairly large variation of the added

*See References

mass does not change the absorbed energy appreciably. See Figure 5, which has been taken from (Analysis).

In a paper by Woisin (1964) the results of different investigators of the added mass are cited. They range from forty to one hundred percent of the actual mass of the struck ship. If the striking ship has twice the displacement of the struck ship,* we find from Figure 5 (corresponding to the above-mentioned range of the added mass) a range from 0.41 to 0.5 for the absorbed energy coefficient. I think that the difference of nearly twenty-five percent (related to the lower value) between the energy coefficients makes it definitely worthwhile to spend some further thoughts on this problem.

In my opinion the most reliable data available at the moment are those given by Motora (1960). He has found them experimentally. For the experiments, eleven different ship models were used. They were developed from a common parent form and cover the following range:

Block coefficient	0.45	through	0.80
Length-beam ratio	5	through	10
Beam-draft ratio	1.8	through	3.6

Three methods have been considered; these are called:

---

*In face of the rapidly increasing number of very big tankers and bulk carriers, this assumption is realistic.

the vibration method, the acceleration method and the impact method after the relationships used to determine the added mass. After some careful preliminary investigation the impact method has been selected for the determination of the added mass for longitudinal translation (this corresponds to the striking ship) and for the added moment of inertia for rotation about the vertical axis. For the determination of the added mass for transversal translation (this corresponds to the struck ship) the acceleration method was found most satisfactory. As an example for the results given by Motora, Figure 6 shows a diagram for the added mass for transverse translations. Similar diagrams are given for the other two cases mentioned above. Finally, the influence of different stern profiles on the added moment of inertia is also given in Motora's paper.

In the experimental tank in Rome, collision experiments have been conducted with the goal of finding added mass data. They are published by Spinelli (1962) and Castagneto (1962). With our present knowledge it is hard to find rational explanations for the results of these experiments. There is not only a wide scatter of the data points but also a dependency of the added mass on the speed of the striking ship. Further, different values have been found for the added mass corresponding to the instant of maximum compression and when the ships just have separated, see Figure 7. It is not very convincing, when one reads in Spinelli's paper, "that it seems to be justified to assume an order of magnitude of 0.35 to 0.5 for the ratio of the added mass of the struck ship to its actual mass." On the other hand the difficulties to explain these experiments make it obvious that our knowledge about the added mass to be used in connection with impacts is not yet satisfactory.

Other collision experiments have been made at the University of Naples, Italy at which a model of the reactor compartment was supported by a car running on rails. Foils submerged in water were attached to the model. In spite of the fact that the area of the foils is equivalent to the lateral submerged area of the ship, I do not think that added mass data found by these experiments can be used for ships. For further information see the papers of Spinelli (1962) and (1964) and also Chapter 1.5.

The theoretical approach of Drittler (1964) and (1966) deals with some mathematical concepts rather than with the hydrodynamics involved. It has yet to be shown if this approach can lead to usable results.

Summarizing, it can be said on the one hand that more information is available now than was during the design of the

SAVANNAH. But on the other hand we still do not understand the problem thoroughly. I am sure that the designers of future collision protections would feel much better if they could lean on more and better information in this field.

1.3 Are Collisions Cases of Absolutely Inelastic Impacts?

Before trying to answer the question raised in the headline I would like to mention the widely divergent opinions expressed in the literature. In the SAVANNAH approach, an absolutely inelastic impact was assumed. On the contrary, Spinelli (1964) and Guida (1964) report coefficients of restitution from 0.64 to 0.85. These rather high values follow from their interpretation of experiments conducted at the Institute of Naval Construction at Naples. The meaning of these coefficents is: Of the total energy absorbed during the period of deformation* about forty to sixty percent is due to elastic deformations and only the rest is used for destruction and plastic deformation of material.

As is shown in Figures 8 and 9, different opinions with regard to the interpretation and evaluation of the experiments mentioned are possible. It is not difficult, for example,

---

*The period of deformation refers to the duration of the collision, starting from the first initial contact of the bodies and ending with the time of maximum deformation. At the end of this period both ships have the same speed.

to get a coefficient of restitution as low as 0.29. Corresponding to this value, less than ten percent of the energy absorbed during the period of deformation is due to elastic deformations. I think this to be much more realistic than the aforementioned high values. Too little is known about the experimental set-up to draw further conclusions.

Castagneto (1962) gives an estimate of the energy which is absorbed by the ship structure as a consequence of the bending of the struck ship in a horizontal plane. His calculations show that this energy is small (see also Chapter 1.4). Similar calculations have been made by Guida (1964). The results are essentially the same as those given by Castagneto (1962). (See also the next chapter.)

I would like to suggest the following answer to the question as to whether ship collisions involve absolute inelasticity:

1. Energy consumption due to elastic deformation of the whole ship (including vibrations) is negligibly small.
2. We do not have to bother about the question whether the impact is absolutely inelastic or not, if we concentrate on the instant of

maximum deflection and penetration. (For this condition, both ships have the same speed.) At that instant the energy contained in the deformed structure is equal to the energy that would be finally absorbed in an absolutely inelastic impact. It can be calculated with the abovementioned equations, taking $e = 0$. It makes no difference for judging the ultimate strength, if energy that is contained in elastically deformed structures is converted into kinetic energy after the striking ship has penetrated the reactor compartment. This concept makes experiments simpler. It goes without saying that the contribution of elastic deformations has to be included when the ultimate ability of a structure to absorb energy is calculated theoretically.

1.4 Longitudinal Bending Moment in a Horizontal Plane

Castagneto (1962) was the first to point out that a collision causes a longitudinal bending moment in a horizontal plane. Later, Guida (1964) and Woisin (1964a and 1964b) also gave thought to this problem.

During a collision, the collision forces (acting in the plane of contact) are in equilibrium with the inertia forces of the ship. The forces try to bend the ship in a horizontal plane (see Figure 10). The amount of the collision force and therefore the resulting bending moment depends on the rigidity of the structure in the region of contact. If the structure collapses at small loads, no big collision force can arise. Most of the energy is dissipated by destroying the structure, which allows the centers of gravity of the ships to move together over a relatively long distance. On the other hand, rigid structures produce big forces. Only little of the energy is dissipated by the deformation of local structures. The result is a big bending moment of the struck ship.

The following table has been calculated in order to give an idea of the magnitude of the collision force and the bending stress. It is based on information given by Castagneto and on the following assumptions: a direct central impact is involved; the collision force is proportional to the change of the distance between the centers of gravity of the ships, starting from the first initial contact; the longitudinal deflection of the ship is proportional to the collision force.

CALCULATION OF COLLISION FORCE, BENDING STRESS AND ENERGY

	Struck Ship	Striking Ship
Mass	m_B = 9200 metric mass tons	m_A = 7000 metric mass tons
Speed	V_B = 0	V_A = 6 m/s

Absorbed energy in the instant when both ships have the same speed:

$$E = \tfrac{1}{2} m_A V_A^2 \frac{m_B}{m_A + m_B} = 71550 \text{ meter-tons (metric)}$$

s meter	F tons (metric)	σ Kg/cm^2	E_1 mt	E_2 mt
8	17800	1320	71200	350
6	23600	1750	70300	650
4	35000	2600	70000	1500
2	66300	4900	66300	5250

s = Maximum change of the distance between the centers of gravity of the ships

F = Collision force

σ = Bending stress

E_1 = Energy absorbed in the region of collision

E_2 = Energy absorbed by longitudinal bending of the struck vessel

The bending moment depends of course on the location of the damage. Woisin (1964a) has investigated the damage location dependency of the collision force that produces a certain maximum bending moment M_{max}. His results are shown in Figure 11. The figure shows that, with regard to this bending moment, the best location of the reactor compartment is about twenty percent of the ship length from the ends of the ship. In preparing the diagram Woisin has assumed a uniform mass distribution over the ship length.

1.5 Planning of Experiments

In order to get useful results from collision experiments, it is necessary to find the relevant laws of similarity. It is hard to understand why this area has been widely neglected; rather expensive experiments have been conducted without sufficient understanding of these laws.

The main difficulty seems to come from a lack of understanding of the two-sidedness of the problem. With the breakdown introduced in this study, however, it is easy to come to a clear understanding. Although this chapter is devoted to the external mechanics of impact, we will also deal with similarity considerations connected with what we have called internal mechanics of impact. With respect to them we can refer to a short chapter in Spinelli (1962). With the notations:

$$\lambda = \text{length ratio}$$

$$\tau = \text{time ratio}$$

$$\mu = \text{mass ratio}$$

we can write the condition for constant density and constant modulus of elasticity for the model and ship:

$$\frac{\mu}{\lambda^3} = 1$$

$$\frac{\mu}{\lambda \tau^2} = 1$$

From this follows:

$$\text{Speed ratio} = \frac{\lambda}{\tau} = 1$$

$$\text{Force ratio} = \frac{\lambda \mu}{\tau^2} = \lambda^2$$

$$\text{Energy ratio} = \frac{\lambda^2 \mu}{\tau^2} = \lambda^3$$

$$\text{Pressure ratio} = \frac{\mu}{\lambda \tau^2} = 1$$

The most important conclusion is that the collision speed used in the experiments has to be the same as the ship speed. With regard to the mass, we have to differentiate between two things: the mass of the involved structure, and the total mass of the two ships. The mass ratio of the structural members of the model and ship in the destruction area has to be $\mu = \lambda^3$. On the other hand, the ratio of the total mass of the model and ship does not have to be

$\mu = \lambda^3$ *. We are completely free to choose, for example, the total mass of the model of the struck ship. It can even approach infinity. (This would be the case, if the model is attached to a big concrete block.) The only thing which we have to do is to make the mass of the model of the striking ship of such a size that the ratio of the energies of the ship and model collision is equal to λ^3 . The following example illustrates this:

Ships Data:

Mass of striking vessel (including added mass)	m_A
Mass of struck vessel (including added mass)	m_B
Speed of striking vessel	V_A
Speed of struck vessel	$V_B = 0$

A direct central impact is assumed.

The energy transferred during the impact is:

$$\Delta E = \tfrac{1}{2} V_A^2 m_A \frac{m_B}{m_A + m_B}$$

For the model the energy is:

$$\Delta E' = \frac{\Delta E}{\lambda^3}$$

*We are neglecting the energy consumption by vibrations, by deformations of the whole ship, etc. It has already been mentioned that these are negligible.

The collision speed for the model has to be equal to the ship speed V_A. We now find the following relationship for the masses m_A and m_B of the models:

$$\Delta E' = \tfrac{1}{2} m_A' V_A^2 \frac{m_B'}{m_A' + m_B'}$$

If, for example, m_B' approximates infinity, we find for m_A':

$$m_A' = \frac{2\Delta E'}{V_A^2}$$

The general relationship for the mass of the striking model is:

$$m_A' = \frac{\Delta E' \, m_B'}{\Delta E' - \tfrac{1}{2} V_A^2 m_B'}$$

In closing this chapter I want to give some comments on experimental set-ups, that are in use in Japan and Italy.* The Japanese test apparatus is shown in Figure 12. It is described in Kagami (1960). The striking ship is simulated by a weight that is supported by two arms. The arms are attached to a tower. The weight carries a model of the bow of the striking ship. The model of the collision protection assembly is attached to a block of

*Until now no details are known of the test apparatus that is being built in Hamburg, West Germany.

concrete. It is therefore necessary to use the abovementioned relationships to determine the size of the weight. The method described in Kagami (1960) for this purpose is wrong and does not provide similarity.

The Italian experimental set-up is shown in Figure 13, which has been taken from Spinelli (1962). The models of the bow and the collision protection assembly are supported by small cars, which can roll on rails. The rails for the striking car have a slope. The car which supports the model of the section of the struck ship has rigidly attached foils submerged in water. The idea in designing this set-up was to reach the closest possible agreement with reality: The mass of both cars can be made equal to the mass of the ships divided by λ^3. The submerged foils were to simulate the effects of the water. In my opinion all this can only impress people who are not familiar with the problem. Otherwise there are a lot of disadvantages connected with the design. We know very little about the added mass of the plates submerged in containers of restricted size. The same is true with regard to wave effects in the containers. The elasticity of the foils also introduces uncertainties rather than a close approximation to reality. More measurements are necessary, and all measurements are more complicated because the struck model is free to move. The examples in Figure 8 and 9 show in a convincing manner the difficulties of evaluating the test results. I am sure that more reliable results can be expected from a set-up where the struck ship is fixed. Further, such a set-up would be cheaper and it would be easier and less expensive to get the needed measurements. It seems to me that the concept of the Italian experiment can only be explained by a lack of understanding the similarity relationships.

2. INTERNAL MECHANICS OF IMPACT

2.1 General

The behavior of ship structure during impacts looks very complex. No wonder that for a long time it was thought impossible to describe it rationally and quantitatively. The designers of the N. S. SAVANNAH deserve credit for refuting this opinion and showing that a quantitative approach is possible.

After this first step was made it was relatively simple to find shortcomings in the method described by Minorsky (1959) and others. However, it seems to be a long way from criticism to improvement. Of some investigations made in other countries, it can be said that they are much more expensive but of less use to the designer of nuclear ships than the method developed for the SAVANNAH.

In my opinion the biggest mistake was to expect a solution of the problems from experiments only. It seems that this has also been realized by Japanese investigators. They started with a purely experimental investigation of eight different designs of collisions protections; see Kagami (1960). The results raise questions rather than answering them. In the following years the same experimental set-up was used for the experimental part of a more systematic approach that started with the investigation of simple, elementary structural elements and was continued with more and more complex structures. A lot of theoretical work was done parallel to the experiments. What has been published until now might not be enough to answer all questions arising during a design. But I think it to be the most promising and fruitful approach available at this time. The following part of this study will therefore be devoted mainly to these Japanese investigations. I will give first a survey of what has been done. Then I will try to draw some conclusions.

For the sake of completeness, however, the experiments being conducted in Naples, Italy, need first be mentioned. As I have already pointed out in Chapter 1.5, there are some shortcomings in the design of these experiments. In addition, the approach is similar to that first tried and then given up in Japan. Therefore I do not expect too much from these experiments. The results to date are reported by Spinelli (1964).

2.2 Investigations of Structural Elements

The following is a survey of (Study 1960, 1961 and 1962). An abstract of (Study 1960 and 1961) has been published in Mitsubishi Nippon Heavy Industries Technical Review 2 (1962), p. 117.

A translation of the abstract is available (BSRA Translation No. 1373).

The experimental set-up which was used by the Japanese investigators has already been described in Chapter 1.5 (see also Figure 12).

(a) Investigation of Beams: The main purpose of this investigation was to establish a theoretical method of calculating the energy absorbed on impact. Four different series of beams supported freely at the ends were tested under static load and under different impact conditions. For this purpose the weight and speed of the striking weight were changed. For the calculations of the absorbed energy the following effects were taken into account:

(1) the effect of strain hardening

(2) the effect of straining speed

(3) the effect of shearing stress

The last effect was found to be negligible. It has been shown that the energy calculated with the following equation is in good agreement with the experimental results:

$$E = \alpha \beta \gamma M_{P_0} \theta$$

where

E = absorbed energy

α = coefficient giving the effect of strain hardening

β = coefficient giving the effect of straining speed

γ = coefficient giving the effect of the shearing stress on the plastic moment

M_{p_o} = plastic moment, based on tensile test results

θ = angle of bend

The average values of the three coefficients are:

$\alpha = 1.16$ $\beta = 1.17$ $\gamma \doteq 1$

Another beam was investigated, which was supported by bolts. This support allowed free movement of the beam around the bolts but restricted the movement in the direction of the beam length. In this case, for the theoretical calculation, the effect of axial stress was also taken into account.

(b) Investigation of Plates: As the result of extensive experimental and theoretical work done on strip plates and square plates the following equation has been suggested for estimating the energy - absorbtion until breaking:

$$E = \alpha m w^* + \frac{1}{2} \gamma n w^{*2}$$

TABLE 1

The formula for estimating total energy absorption

$$E=\alpha\cdot m\cdot w^{*}+\frac{1}{2}\cdot\gamma\cdot n\cdot w^{*2}$$

E : Total energy absorption until breaking.
w^* : Deflection at time of destruction.
m : Collapse load in bending.
n : Constant concerning membrane effect.
α : Constant concerning influence of strain rate, $\left(\frac{d\varepsilon}{dt}\right)_\alpha$.
γ : Constant concerning influence of strain rate. $\left(\frac{d\varepsilon}{dt}\right)_\gamma$.

Types of Model		Scantling of Stiffener h×Tmm	m	n	$\left(\frac{d\varepsilon}{dt}\right)_\alpha$	$\left(\frac{d\varepsilon}{dt}\right)_\gamma$	w^*
Strip Plate Model	K	—	0	$\frac{4\cdot b\cdot t\cdot\sigma_y^*}{l}$	0	$\frac{\varepsilon^*\cdot V}{2\cdot w^*}$	$\sqrt{\frac{\varepsilon^*}{2}}\cdot l$
	L	40×4.5	$\frac{8M_P}{l}$	$\frac{4\cdot b\cdot t\cdot\sigma_y}{l}$	$\frac{h\cdot V}{d\cdot l}$	$\frac{w^* V}{l^2}$	—
		80×2.3	$\frac{4M_P}{l}$				
Panel Model	M	—	0	$\frac{2\pi t\sigma_y}{\log_e\frac{l}{2r_e}}$	0	$\frac{4\cdot k\cdot r_e^2\cdot V}{l^2\cdot w^*}$	$k\cdot r_e\cdot\log_e\frac{l}{2r_e}$
	N	40×4.5	$\frac{16M_P}{l}$	$\frac{2\pi t\sigma_y}{\log_e\frac{l}{2r_e}}$	$\frac{h\cdot V}{d\cdot l}$	$\frac{4\cdot k\cdot r_e^2\cdot V}{l^2\cdot w^*}$	$k\cdot r_e\cdot\log_e\frac{l}{2r_e}$
		80×2.3	$\frac{8M_P}{l}$				
	P	40×4.5	$\frac{32M_P}{l}$	$\frac{2\pi t\sigma_y}{\log_e\frac{l}{4r_e}}$	$\frac{h\cdot V}{2d\cdot l}$	$\frac{16\cdot k\cdot r_e^2\cdot V}{l^2\cdot w^*}$	$k\cdot r_e\cdot\log_e\frac{l}{4r_e}$
		80×2.3	$\frac{16M_P}{l}$		$\frac{5h\cdot V}{6d\cdot l}$		

M_P : Full plastic moment of one beam
l : Span
V : Impact velocity
d : Extent of plastic hinge
r_e : Radius of loading area in panel model
σ_y : Yield stress

$$\sigma_y^*=\begin{cases}\sigma_y & \text{(Without effect of strain-hardening)}\\ (\sigma_y+\sigma_{max})/2 & \text{(Including effect of strain-hardening)}\end{cases}$$

$\varepsilon^*=0.25$
$k=0.89$

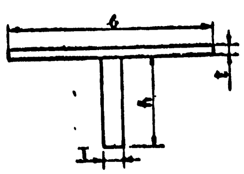

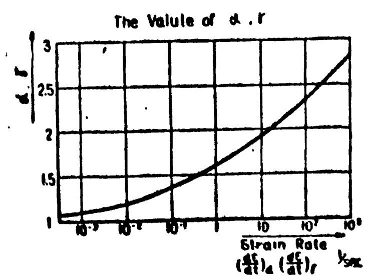

TABLE 2

Energy absorption until breaking

Model	Load	Energy absorption T-M*		
		Fxperimental	Calculated	Ratio
K10-0	Statical	1.724	1.233	1.398
	〃	〃	1.612※	1.069
K20-0	Statical	2.650	1.977	1.342
	〃	〃	2.415※	1.099
K20-1⊗	Impact	0.966	0.932	1.036
	〃	〃	1.143※	0.845
K20-2⊗	〃	1.362	1.164	1.170
	〃	〃	1.427※	0.955
L11-0	Statical	0.335	0.285	1.179
L11-1	Impact	0.427	0.416	1.025
L11-2	〃	0.269	0.250	1.075
L21-0	Statical	0.499	0.525	0.951
L21-1	Impact	0.801	0.825	0.971
L21-2	〃	0.653	0.804	0.813
L12-0	Statical	0.633	0.504	1.256
L12-1⊗	Impact	0.579	0.567	1.019
L12-2⊗	〃	0.577	0.567	1.006
L22-0	Statical	1.690	1.260	1.340
L22-1	Impact	0.911	0.725	1.256
L22-2	〃	0.944	0.788	1.198
M10-1	Impact	0.407	0.293	1.387
M10-2	Statical	0.257	0.215	1.194
M20-0	Statical	0.315	0.311	1.012
M20-1	Impact	0.449	0.426	1.053
M20-2	〃	0.399	0.418	0.955
M30-0	Statical	0.483	0.433	1.114
M30-1	Impact	0.744	0.598	1.243
N11-1	Impact	0.631	0.565	1.118
N11-2	Statical	0.505	0.360	1.400
N21-0	Statical	0.571	0.480	1.190
N21-1	Impact	0.781	0.742	1.152
N21-2	〃	0.734	0.727	1.009
N12-1	Impact	0.603	0.564	1.072
N12-2	Statical	0.459	0.347	1.323
N22-0	Statical	0.567	0.453	1.252
N22-1	Impact	0.692	0.724	0.943
N22-2	〃	0.665	0.694	0.955
P21-1	Impact	0.766	0.753	1.009
P21-2	Statical	0.517	0.457	1.130
P22-0	Statical	0.475	0.445	1.068
P22-1	Impact	0.650	0.812	0.801
P22-2	〃	0.678	0.775	0.876

⊗ Since no breaking occurred. the energy absorption shows the value till maximam deflection.
※ Including effect of strain hardening.
* T-M = meter-tons

TABLE 3

Types and scantlings of models

MARK			PLATE		STIFFENER		LOAD
			SCANTLING	THICKNESS	SCANTLING	NUMBER	
STRIP PLATE MODEL	K TYPE	K10- 0	700×175	1.6			STATICAL LOAD
		K10- 1	〃	〃			IMPACT
		K10- 2	〃	〃			IMPACT
		K20- 0	〃	2.3			STATICAL
		K20- 1	〃	〃			IMPACT
		K20- 2	〃	〃			IMPACT
	L TYPE	L11- 0	〃	1.6	40×4.5FB	1	STATICAL
		L11- 1	〃	〃	〃	〃	IMPACT
		L11- 2	〃	〃	〃	〃	IMPACT
		L21- 0	〃	2.3	〃	〃	STATICAL
		L21- 1	〃	〃	〃	〃	IMPACT
		L21- 2	〃	〃	〃	〃	IMPACT
		L12- 0	〃	1.6	80×2.3FB	〃	STATICAL
		L12- 1	〃	〃	〃	〃	IMPACT
		L12- 2	〃	〃	〃	〃	IMPACT
		L22- 0	〃	2.3	〃	〃	STATICAL
		L22- 1	〃	〃	〃	〃	IMPACT
		L22- 2	〃	〃	〃	〃	IMPACT
PANEL MODEL	M TYPE	M10- 0	700×700	1.6			STATICAL
		M10- 1	〃	〃			IMPACT
		M10- 2	〃	〃			IMPACT
		M20- 0	〃	2.3			STATICAL
		M20- 1	〃	〃			IMPACT
		M20- 2	〃	〃			IMPACT
		M30- 0	〃	3.2			STATICAL
		M30- 1	〃	〃			IMPACT
		M30- 2	〃	〃			IMPACT
	N TYPE	N11- 0	〃	1.6	40×4.5FB	1 × 1	STATICAL
		N11- 1	〃	〃	〃	〃	IMPACT
		N11- 2	〃	〃	〃	〃	STATICAL
		N21- 0	〃	2.3	〃	〃	STATICAL
		N21- 1	〃	〃	〃	〃	IMPACT
		N21- 2	〃	〃	〃	〃	IMPACT
		N12- 0	〃	1.6	80×2.3FB	〃	STATICAL
		N12- 1	〃	〃	〃	〃	IMPACT
		N12- 2	〃	〃	〃	〃	STATICAL
		N22- 0	〃	2.3	〃	〃	STATICAL
		N22- 1	〃	〃	〃	〃	IMPACT
		N22- 2	〃	〃	〃	〃	IMPACT
	P TYPE	P21- 0	〃	2.3	40×4.5FB	3 × 3	STATICAL
		P21- 1	〃	〃	〃	〃	IMPACT
		P21- 2	〃	〃	〃	〃	STATICAL
		P22- 0	〃	〃	80×2.3FB	〃	STATICAL
		P22- 1	〃	〃	〃	〃	IMPACT
		P22- 2	〃	〃	〃	〃	IMPACT

The meaning of the symbols is explained in Table 1, p. 26. A comparison of the experimental results and those of calculations is given in Table 2, p. 27. The types and scantlings of the models are shown in Table 3, p. 28. As can be seen from Table 2 the agreement between the experimental and theoretical results is in most cases good enough for practical purposes. Figure 14 is a typical example for the load - deflection relationship. The difference between static and dynamic loads and between different dynamic loads (see Table 2) should be noted.

Of great interest is the comparison of the behavior of mild steel and high tensile steel plates. The types and scantlings of the investigated models are given in the following table.

TABLE 4

Types and Scantlings of Models

Mark	Plate			Stiffener		
	Scantling	Thickness	Material	Scantling	Number	Material
M1A	700x700	1.6	M S			
H1A	"	"	H T			
M1B	"	2.3	M S			
H1B	"	"	H T			
M2C	"	3.2	M S	40x4.5F B	1x1	M S
H2C	"	"	H T	"	"	"
M3B	"	2.3	M S	"	3x3	"
H3B	"	"	H T	"	"	"

Figure 15 shows the load under impact plotted against the deflection. The high tensile steel plates absorb more energy per unit deflection and their breaking load is bigger. On the other hand, the absorbed energy until rupture is much higher in the case of mild steel plates. Table 5 gives the ultimate absorbed energy and, for a fair comparison, the energy absorbed per unit thickness.

TABLE 5

Energy absorption until breaking

Model	Condition	Energy absorption	Energy Absorption per unit thickness
M 1 A	*	.169 t-m	.111t-m/mm
H 1 A	To breaking	.191	.108
M 1 B	*	.410	.155
H 1 B	To breaking	.330	.136
M 2 C	"	.683	.212
H 2 C	"	.496	.147
M 3 B	"	.437	.172
H 3 B	"	.375	.154

In models marked *, no crack occurred

These results do not as yet allow one to decide which material should be preferred for collision protection. Some further comments will be given later (see Chapter 2.4).

2.3 Investigations of Models of Ship Sides and Ship Bows

The following is a survey of (Study 1963). An extract of this report has been published in the Journal of Zosen Kiokai, Vol. 115, Dec. 1965, p. 259. A translation of (Study 1963) is being prepared in connection with the present survey and should be submitted shortly.

The investigated models of ship sides are shown in Figures 16 and 17. The design of the bow models is given in Figure 18 and 19.

TABLE 6

Bow Model	Side Model			Test	
	Type	Thickness of side shell	Thickness of deck plate	Static	Impact
B-1(Solid)	S 1-1	2.3	0.7	X	X
	S 1-2	1.6	1.2	X	X
	S 1-3	1.0	1.6	X	X
	S 2-1	2.3	0.6	X	X
	S 2-2	1.6	1.2	X	X
B-2(Soft)	S 1-1	2.3	0.7	X	X
	S 1-2	1.6	1.2	X	X
	S 2-1	2.3	0.6	X	X
	S 2-2	1.6	1.2	X	X
B-2 (Soft)	Solid Wall	---	---	X	X
B-2'(Soft)	"	---	---	X	---
B-2"(Soft)	"	---	---	X	---

Table 6 contains a summary of the tests and gives also the thickness of the side shell and deck plates of the models of the ship side. As can be seen from the table, the side models have been struck with solid bows and the bow models have been tested against a solid wall. The purpose of these experiments has been to find experimental data which are comparable to calculated data. Figure 20 gives an example of the obtained results. It shows good agreement between the calculated and the experimentally established load-deflection curve. The practical use of these investigations will be shown later.

The case of a collision between the models of a bow and a side structure is much more complicated than the case in which one of the collision partners is solid. The impact force is not uniformly distributed over the ship side and the stem respectively. It concentrates in the neighborhodd of the stiffer members of the structure as for example decks. Because the stiffened regions of the side structure practically never coincide with those of the bow, the force which causes the breakdown of the structure is lower. This is illustrated in Figure 21 and 22. In these figures the dashed curves correspond to tests with solid counterparts. As it can be seen, the ultimate load in this case is much higher than in the case of two soft models.

The impact tests have also shown another interesting result. A closer inspection of Figures 21 and 22 shows that the load-deflection relationship is different in the two cases represented by these figures. In Figure 21 the load first increases on both the bow and the side structure. After buckling of the bow has been initiated, the load decreases. At the same time the deformation of the bow is continuing, whereas the deflection of the side structure remains constant. Than the load increases again, causing further deformation of the bow, but not changing the deflection of the side structure. In Figure 22 the initial behavior of the load and deflection of the bow and of the side structure are the same as in the former case. A difference shows up when the maximum load is reached. The load is limited in this case by the breaking of the shell. After the maximum load has been reached it decreases rapidly; the deflections keep about the same value reached in the instant of maximum load.

According to the findings of all the experiments made* it can be predicted whether the behavior of the structures will be similar to that shown in Figure 21 or to that shown in Figure 22. If the ultimate strength of the bow, when colliding with a solid wall, is higher than the ultimate strength of the ship side struck with a solid bow, then the shell will break before buckling the bow.

*The Japanese researchers do not restrict the following conclusions to the experiments made; they think they hold generally.

The behavior of the structures is then similar to that shown in Figure 22. If the strength of the ship side is higher than the strength of the bow, both of them tested with a solid counterpart, than the behavior will be similar to that shown in Figure 21.

Although the four impact tests suggest the aforementioned rule, and contrary to the opinion of the Japanese researchers, I am not yet sure that it will hold in all cases. I would regard it rather as a hypothesis that still has to be proved. I am suspicious not only because of the small number of structures tested, but also because I feel that a relatively wide random scatter has to be expected in this kind of experiment. It is easy to imagine that it is difficult to build two models which are so alike, that they actually have the same strength.

The absorbed energy is of course equal to the sum of the areas under the load-deflection curves of the bow and of the side structure.

2.4 Some Preliminary Conclusions from the Tests with Ship Structures

The results of the tests reported in the foregoing chapter suggest some thoughts about their interpretation and applicability. But before doing this I would like to stress the fact that it is impossible to reach any final conclusions with the knowledge which is as yet available. What I hope can be done is to stimulate a new approach to some questions, which might be useful in the future.

At the end of paragraph (b) of Chapter 2.2 some further comments on the relative merits of high tensile and mild steel were foretold, and these now follow. The conclusions drawn by the original investigators of this problem are not satisfactory. They say: "The absorbed energy per unit deflection is more favorable to the high tensile steel plate. However, the absorbed energy up to rupture is not favorable to high tensile steel plate due to its small elongation." With this result it is impossible to answer the question: Is high tensile steel or mild steel to be preferred for collision protection structures? We need therefore a decision procedure that includes more information than that contained in the test results and leading to the ambiguous statement that both materials have their advantages and disadvantages.

In order to sketch such a decision procedure it is necessary to extrapolate some of the findings reviewed in the foregoing chapters. If future investigations should show that the extrapolations are wrong I think it will not be too difficult to change the procedure so that it takes account of the latest state of knowledge. Further, it is likely that the procedure will have to be extended in the one direction or the other in order to take care of influences that are not known at the moment.

Assume we want to compare a mild steel structure and a high tensile steel structure. The ultimate strength of these structures and of the bow of the striking vessel are assumed to have the following order:

$$P_B < P_M < P_H$$

where

P_B = ultimate strength of the bow of the striking vessel

P_M = ultimate strength of the mild steel side structure

P_H = ultimate strength of the high tensile steel side structure

The relationship $P_M < P_H$ is hypothetical; its assumption is based on the experiments described in Chapter 2.2(b) of this study (see also Figure 15). From what has been said in Chapter 2.3, we conclude that in a collision with either of the side structures the bow will collapse and absorb the energy E_B. The side structures will also absorb some energy before the collasped bow intrudes into the reactor compartment. Extrapolating the test results with mild steel and high tensile steel plates we assume, that

$$E_M > E_H$$

where

E_M = maximum energy which can be absorbed by the mild steel structure,

E_H = maximum energy which can be absorbed by the high tensile steel structure

in both cases, before the reactor is hit.

The total energy which can be absorbed without hitting the reactor is $E_B + E_M$ in the case of mild steel side structure and $E_B + E_M$ in the case of high tensile steel side structure. From the foregoing follows:

$$E_B + E_M > E_B + E_H$$

This means that in this case the mild steel structure is more favorable.

Next we assume another striking ship, but the same side structures as before so that the order of the ultimate strength is:

$$P_M < P_B < P_H$$

Now in a collision with the mild steel structure the bow is not expected to collapse. It will therefore absorb only a small amount of energy E_{BM}. On the other hand, when striking the high tensile structure we expect (according to what has been said in Chapter 2.3) the bow to collapse and to absorb the energy E_{BH}. E_{BH} is of course greater than E_{BM}. In this case the ultimate energy E_M^* which can be absorbed by the mild steel structure can not be much higher (if it is higher at all) than the ultimate energy E_H^* which can be absorbed by the high tensile structure, because the uncollapsed bow finds less resistance than the collapsed one. Therefore it might well be that in this case the unequality

$$E_{BM} + E_M^* \angle E_{BH} + E_H^*$$

comes true. This means, that the high tensile steel structure is more favorable.

Similar considerations can be made for a bow with an ultimate strength which is higher than the strength of both the mild steel and high tensile steel side structure.

It might seem that we have not made much progress: As before we have found, that both the mild steel and the high tensile steel structure have their advantages. But we can now also state, that it depends on the circumstances which one is more favorable. A somewhat closer view of the circumstances might therefore be of use. We have found that the ultimate strength of the bow of the striking vessel and the total impact energy (which for a given struck ship depends on the size and speed of the striking vessel and the location of the impact) are of influence. We can now draw a diagram, which shows the impact energy on the horizontal axis and the ultimate strength of ship bows on the vertical axis, see Figure 23. In the diagram we can mark the ultimate strength of a bow that **is** equal to the ultimate strength of the side structure (for example P_M for the mild steel structure). Further, we can draw into the diagram the energy that can be absorbed before the reactor compartment is penetrated. As explained above this energy depends on the strength of the bow of the striking vessel. If the ultimate strength of the bow is lower than that of the side structure, the absorbed energy is higher than in the reverse case. The absorbable energy is therefore a stepped vertical line in Figure 23. For combinations of P_B and E on the righthand side of the line penetration of the reactor is to be expected.

The next step is to find the probability, with which certain combinations of P_B and E may occur. For this purpose, the probability density, $f_1(P_B)$ must first be established. Then, for each P_B (or in other words for each ship) the conditional probability density $f_2(E|P_B)$ -- which indicates the probability of the occurrence of E if P_B is given -- has to be determined. (The latter probability idea was used in the SAVANNAH analysis). The joint probability density is then

$$f(P_B, E) = f_1(P_B) \cdot f_2(E|P_B)$$

With this we find for the probability that the reactor compartment is penetrated:

$$\text{Prob} = \iint_{D} f(P_B, E)\, dP_B \, dE$$

The integral is to be taken over the domain D which is shown in Figure 23. The probability density $f(P_B, E)$ is of course independent from the collision protection structure. But in general the domain D will be different for different structures. Different structures are therefore characterized by different probabilities that the reactor compartment gets penetrated. With these probabilities we have a basis not only to decide which is the best of two or more structures. We have also a scale to measure the merits of the individual structures.

In the foregoing, a decision between mild steel and high tensile steel structures is used as an example. I expect that the situation will be similar when we have to compare other structures. Finally, I would like to mention, that the probability $P(D) \cdot P(E)$ used in (Analysis, page 139) can be regarded as a special case of the method described here.

The estimation of $f(P_B, E)$ should have been dealt with in the following Chapter 3. Because of the complete lack of data this was not possible and I have to restrict myself to mentioning the problem.

3. STOCHASTIC ASPECTS OF COLLISIONS

3.1 General

An able study of the probability of reactor system damage in collision has been given in Chapter V of (Analysis). I am convinced that this probability is one of the fundamental items of informations necessary to judge the safety of nuclear ships. Especially with view to a greater number of nuclear ships in the future, such an approach is the only way to make valid comparisions of the safety of ships of different size and design. It is therefore also an important prerequisite for logical and sensible safety regulations.

It is regrettable that the probability approach has been neglected. Since the SAVANNAH design, no technical paper has been devoted to the topic.*) This may be because it is still a strange field to most naval architects and marine engineers. Some educational progress may be stimulated by the work of the IMCO (Intergovernmental Maritime Consultation Organization). There, a stochastic approach is used for studying the subdivision of ships with regard to their safety in the case of collisions and groundings. In spite of the different aim of these investigations, it seems worthwhile to mention here some of the results of a collection of damage data initiated by IMCO. The survey given in Chapter 3.2

*) Except an able discussion of it in (Criteria).

promotes a better understanding of the general problem. It also gives some suggestions as to how the data collected by the IMCO could be used for information pertinent to collision protection of nuclear powered ships.

3.2 Statistics of Damage of Conventional Ships

Some years ago IMCO asked its members for information on ship casualities. The collected data has been evaluated by the Federal Republic of Germany. The following is taken from a document of IMCO (1964), private information submitted by Dipl. Ing. W. Riepe, and from papers by W. Riepe (1965) and O. Krappinger (1964).

(a) Distribution of damage length and penetration: Theoretical considerations have led to the hypothesis that the length as well as the penetration of damage from collisions are approximately log-normally distributed. With the data submitted by IMCO, the validity of this hypothesis could be proved. Figure 24 shows schematically the distribution density and the distribution function of the log-normal distribution. This distribution shows that relatively small damages are most likely. It can also be concluded from this distribution that only a small percentage of collisions are really serious.

(b) Penetration of damage: Figure 25 shows the distribution functions of the penetration of damage for ships with lengths of less, and of more than 100 meters (about 300 feet). It can be seen, that big penetrations are more likely to occur in big ships. This is also shown by the relationship between the mean of the penetration (b) and the breadth of the ship (B):

$$b = 0.24B - 0.20 \quad \text{(b and B in meters)}$$

It can be concluded that big ships are likely to be involved in collisions with other big ships. If the composition of the population of the striking ships would be the same for big and small vessels, the penetrations into the big ships would be smaller because of their greater structural strength. It would be of interest to use the data collected by IMCO to establish a statistical relationship between the size of the struck and striking vessels.

(c) Location of damage: Figure 26 is a histogram showing the frequency with which the center of the damage occurs in different ranges of the ship's length. It can be seen that the forward part of the ship is more likely to be hit than the after part.

(d) Size of damage versus location of damage: The knowledge of the frequency of damages at different points of the ship's length is not enough to find the location of the reactor compartment which is optional with respect to the collision protection. For this purpose it is also necessary to have some information on the energy which has to be absorbed at different ranges of the ship's length. If we assume that greater energy corresponds to greater damage length, we can use Figure 27 for this purpose. It shows the median of the damage length versus the ship's length. Because of the relatively small number of data available the estimated medians are subject to random scatter. The "real" value of the median can be expected to be covered by the shown intervals with a probability of ninety percent. Taking this into account we can conclude from Figure 27 that only over the after quarter of the ship's length, substantial lighter collision are to be expected. It would be useful to make a similar evaluation in order to find the dependency between the penetration and the location of damage.

4. IDEAS AND SUGGESTIONS FOR PROTECTION STRUCTURES

A collection of some ideas on the design of collision protection is given in the following. On the one hand they may serve to stimulate the designers of future protection structures. On the other hand, they are a good example to show how far we still are from a rational evaluation of the merits of the individual designs. It is true that some of the structures which will be mentioned in the following have been tested. But the impact energy used at these tests has been so low that the results (the deflections of the ship sides) are not significant for the ultimate strength of the different structures. The latter consideration is much more important than the rather small deflections caused by light impacts.

The Figures 28 through 35 are taken from the paper by Kagami (1960). Figure 36 represents an English suggestion; it has been taken from Woisin (1964a). Figure 37 comes from Spinelli (1961). Because it represents a ship which is being built, the collision protection structure of the West German nuclear research vessel is thought to be of some interest. It is shown in Figure 38. A brief description of the features of the shown structures is given in the following.

The structures in Figures 28 through 35 have been designed for equal weight. Comparing Figures 28 and 29 it can be seen that the structure shown in the latter has a lighter shell, but wider horizontal girders. The structure in Figure 30 has a thinner shell and wider web frames than that in Figure 28. In Figure 31 there are pipes provided near the side shell. Figure 32 shows a structure with a double side shell. A similar idea has been used in the case shown in Figure 33. A longitudinal bulkhead is located between the side shell and the reactor compartment. Swash bulkheads are alternately attached to its inner and outer side. The structure in Figure 34 and 35 is characterized by horizontal members, which are connected with the side shell and the wall of the reactor compartment.

The structure in Figure 36 consists of vertical girders connected alternately to the side shell and the wall of the reactor compartment. There are also decks between the side shell and the reactor compartment and, between them, horizontal girders which are attached to the vertical girders. The idea on which the structure in Figure 37 is based is to provide "knives" which help to destroy the bow of the striking ship.

The collision protection structure of the West German research vessel (Figure 38) consists of three decks in the side tank, which are alternately connected to the side shell and the reactor wall and with the inner sides of the vertical girders.

BIBLIOGRAPHY

1. References Used for this Study

(Analysis): N. S. SAVANNAH Safety Assessment, Vol. IV, Analysis of Hypothetical Accidents. AEC and MARAD 1960.

Castagneto, E. (1962): "L'energia distruttiva nella collisione della navi," Tecnica Navale, 1962, p. 731-742.

(Criteria): Criteria for Guidance in the Design of Nuclear Powered Merchant Ships by Gibbs and Cox, Inc., Maritime Administration, Washington, D. C., May 1961.

Drittler, K. (1964): "Halbempirische Bestimmung der hydrodynamischen Kenngrössen bei Schiffskollisonen," Jahrbuch der Studiengellschaft zur Förderung der Kemenergieverwertung in Schiffbau und Schiffahrt e.V. 1964, p. 169-171.

Drittler, K. (1966): "Die Bestimmung von hydrodynamischen Kenngrössen bei Schiffsbewegungen parallel zur Wasseroberfläche und bei Kollisionen," Schiffstechnik, 1966.

Guida, A. (1964): "Analisi della similitudine nella prove di collisione," Tecnica Italiana, 1964, p. 213-222.

IMCO (1964): Document SES 111/9/App. 1, May 1964: Statistical Analysis of Casualities to Ship Hull. Prepared by Lehstuhl für Entwerfen von Schiffen am Institut für Schiffbau der Universität Hamburg.

Kagami, K. et al. (1960): "Research on the Collision-resisting Construction of Ship's Sides," Symposium on Nuclear Ship Propulsion, Taormina, Italy 1960.

Krappinger, O. (1964): "Über Leckverteilungen," Schiffstechnik 1964, p. 67-98.

Minorsky, V. U. (1959): "Analysis of Ship Collisions with Reference to Protection of Nuclear Power Plants," Journal of Ship Research 3, 1959, p. 1.

Riepe, W. (1965): "Leckstatistik", Hansa 1965, p. 1371-1372

Spinelli, F. (1961): "Sulla protezione anticollisione delle navi a propulsione con energia nucleare", Tecnica Italiana, November 1961.

Spinelli, F. (1962): "Defense des reacteurs nucleaires de navire contre les abordages", A.T.M.A., 1962, p. 281-300.

Spinelli, F. (1963): "La sicurezza del reattore nucleare a bordo delle navi merchantili", Tecnica Italiana, December 1963.

Spinelli, F. (1964): "Protection di compartiment di reacteur nucleaire contre les abordages reacteurs d' essais sur modeles", A.T.M.A., 1964, p. 727-751.

(Study 1960): Study under the government's research contract for peaceful uses of atomic energy for 1960 fiscal year, Jap. Soc. of Research on Nucl. Ships, Tokyo, Japna 1960.

(Study, 1961): Study under the government's research contract for peaceful uses of atomic energy for 1960 fiscal year, Jap. Soc. of Research on Nucl. Ships, Tokyo, Japan 1961

(Study 1962): Study under the government's research contract for peaceful uses of atomic energy for 1960 fiscal year, Jap. Soc. of Research on Nucl. Ships, Tokyo, Japan 1962

(Study 1963): Study under the government's research contract for peaceful uses of atomic energy for 1960 fiscal year, Jap. Soc. of Research on Nucl. Ships, Tokyo, Japan 1963.

Woisin, G. (1962): "Der Einfluß des Drehimpulses bei einer Schiffskollision besonders im Hinblick auf die Sicherheit von Atomschiffen", Schiff und Hafen 1962, p. 577-581.*

Woisin, G. (1964a): "Kollisionspronbleme bei Atomschiffen", Hansa 1964.

---

*Has been translated into English (Marad 3/26/65)

Woisin, G. (1964b): "Fragen des Kollisonsschutzes bei Reactorschiffen", Jahrbuch der Studiengesellschaft zur Forderung der Kernenergiev erwertung in Schiffbau und Schiffahrt e.V. 1964, p. 169-171.

2. References Not Directly Related to Collision Protection

Argiero, L.: "L'inquinamento radioattivo del mare (The radioactive pollution of the sea). Tecnia Italiana, Part I: December 1962, Part II: January/February 1963.

Castagneto, E.: "Carene per navi nucleari" (Hulls for nuclear ships). Tecnica Italiana, Part I: April 1962, Part II: May 1962.

Fasano, E.: "Nota preliminare sulla robustezza delle navi a propulsione nucleare (Preliminary report on the strength of nuclear ships.) Tecnica Italiana, January/February 1962

Fasano, E. and di Biase, A.: "Problemi di sicurezza della nave a propulsione con energia nucleare visti dall'ingegnere navale-meccanico" (Problems of the safety of nuclear ships from the point of view of marine engineers). Tecnica Italiana, August 1962.

Spinelli, F. and de Biase, A.: "Schema di regolamento per la costruzione delle navi nucleari" (considerations on regulations for the design of nuclear ships). Tecnica Italiana, March 1963.

Spinelli, F. et al.: "Rilievi accelerometrici a bordo di grandi navi" (Measurements of the accelerations on load of big vessels). Tecnica Italiana, May 1964.

Woisin, G., "Abschatzung der durch Schiffskollisionen hervorgerufenen Beschleunigunjen", Schiff und Hafen 1961, p. 1021-1023 and 1962, p. 510.

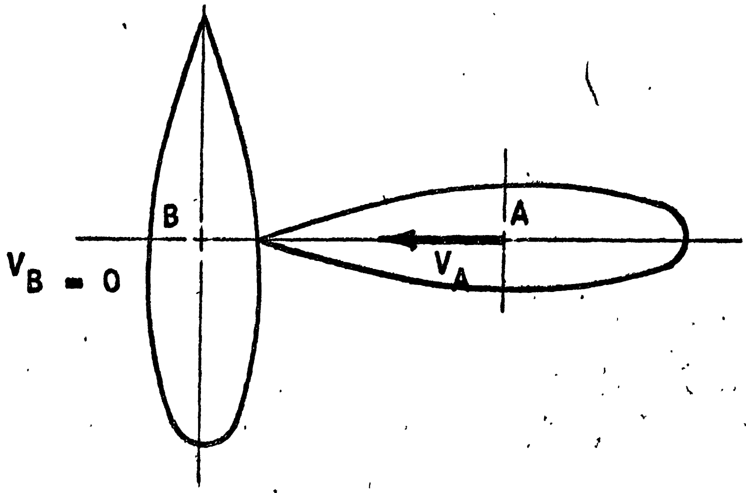

FIGURE 1 - Case 1: Direct Central Impact

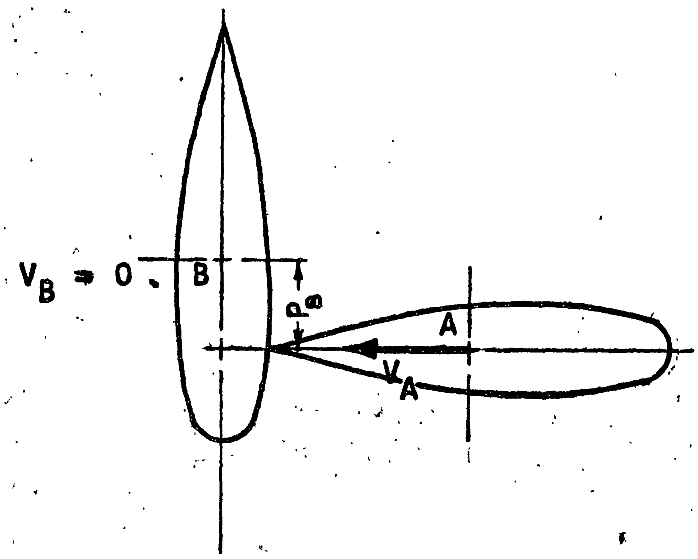

FIGURE 2 - Case 2: Direct Eccentric Impact

FIGURE 3 - Case 3: Oblique Central Impact

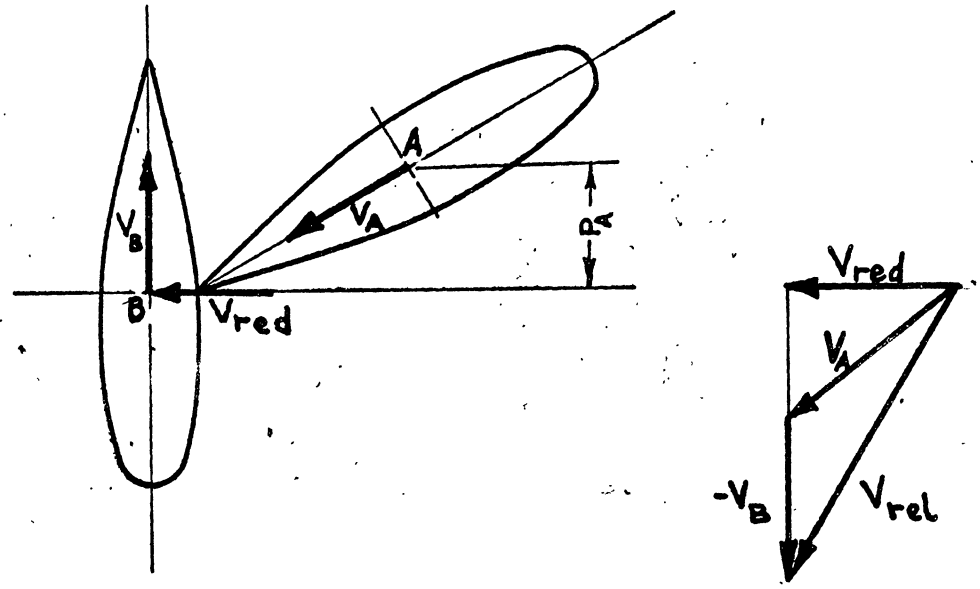

a) Assumption of forces normal to the plane of contact only

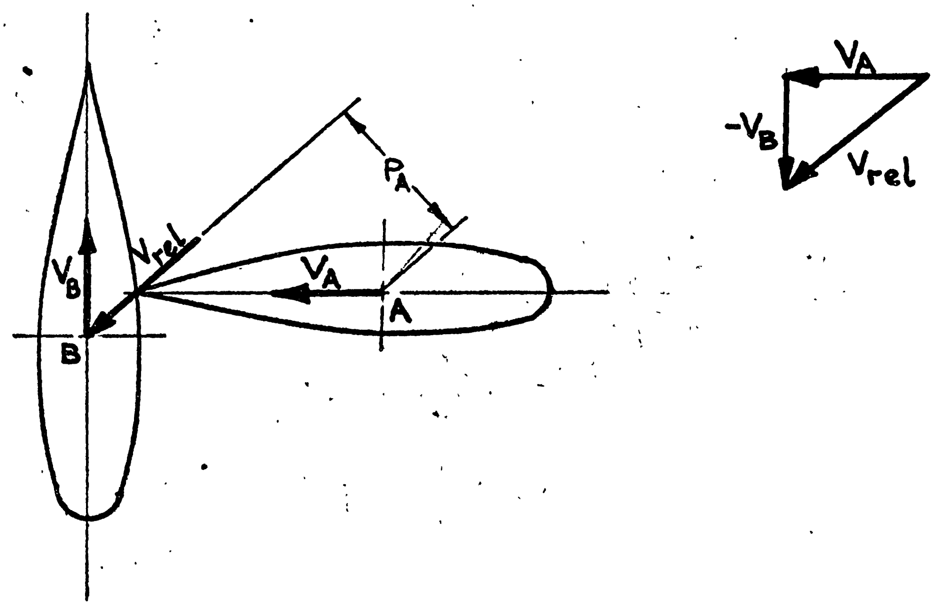

b) Assumption of forces colinear with the relative speed

FIGURE 4 - Case 4: Oblique Eccentric Impact

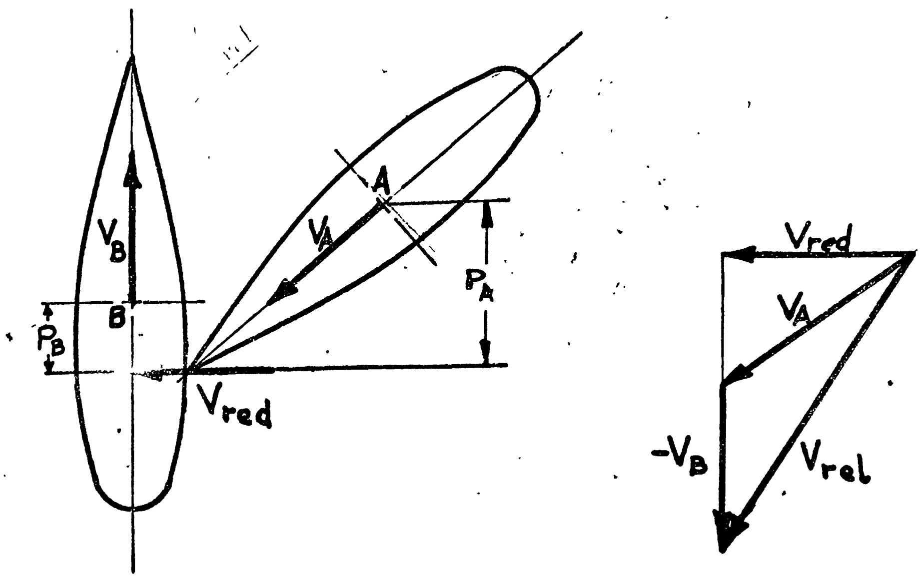

a) Assumption of forces normal to the plane of contact only

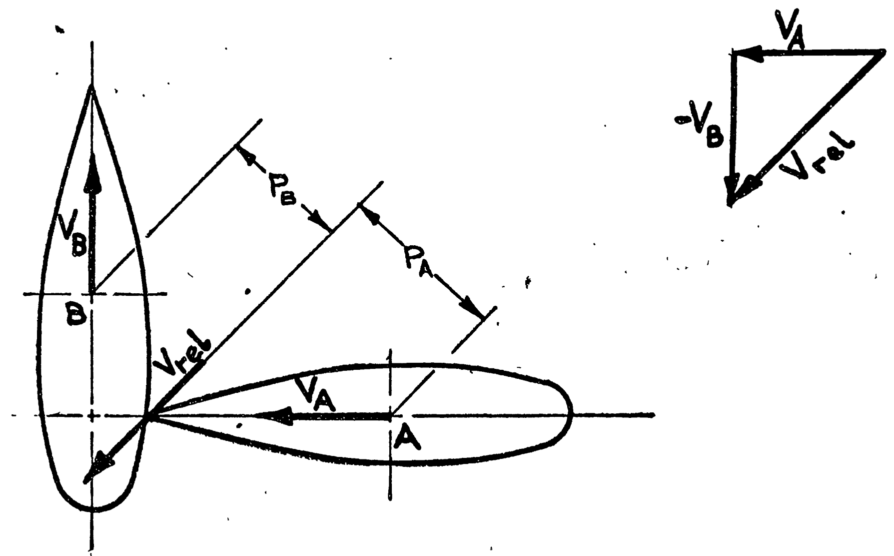

b) Assumption of forces colinear with the relative speed

FIGURE 5

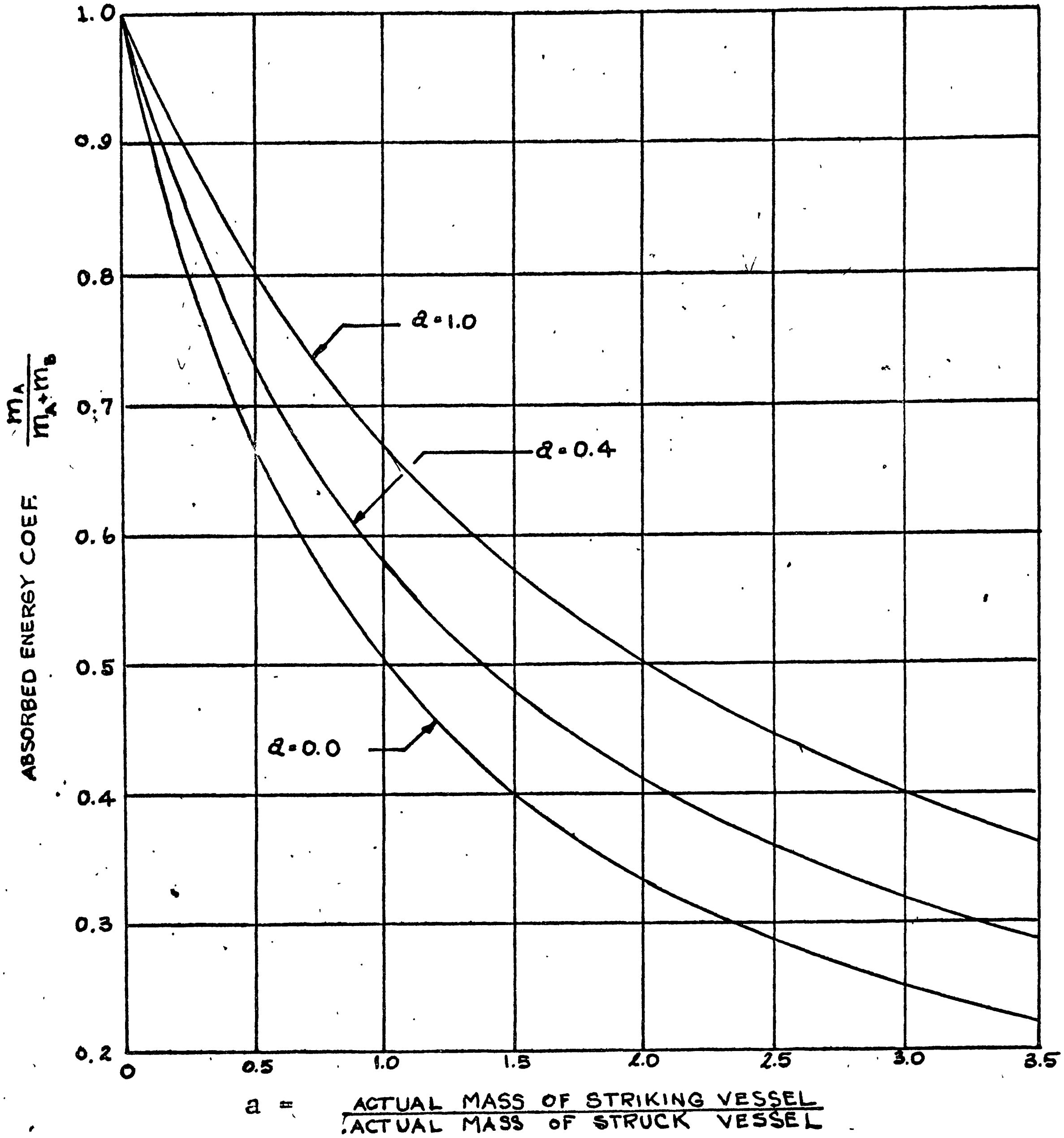

$$a = \frac{\text{Added mass of the struck vessel}}{\text{Actual mass of the struck vessel}}$$

Other notations as defined in the text.

This figure is taken from (Analysis)

FIGURE 6

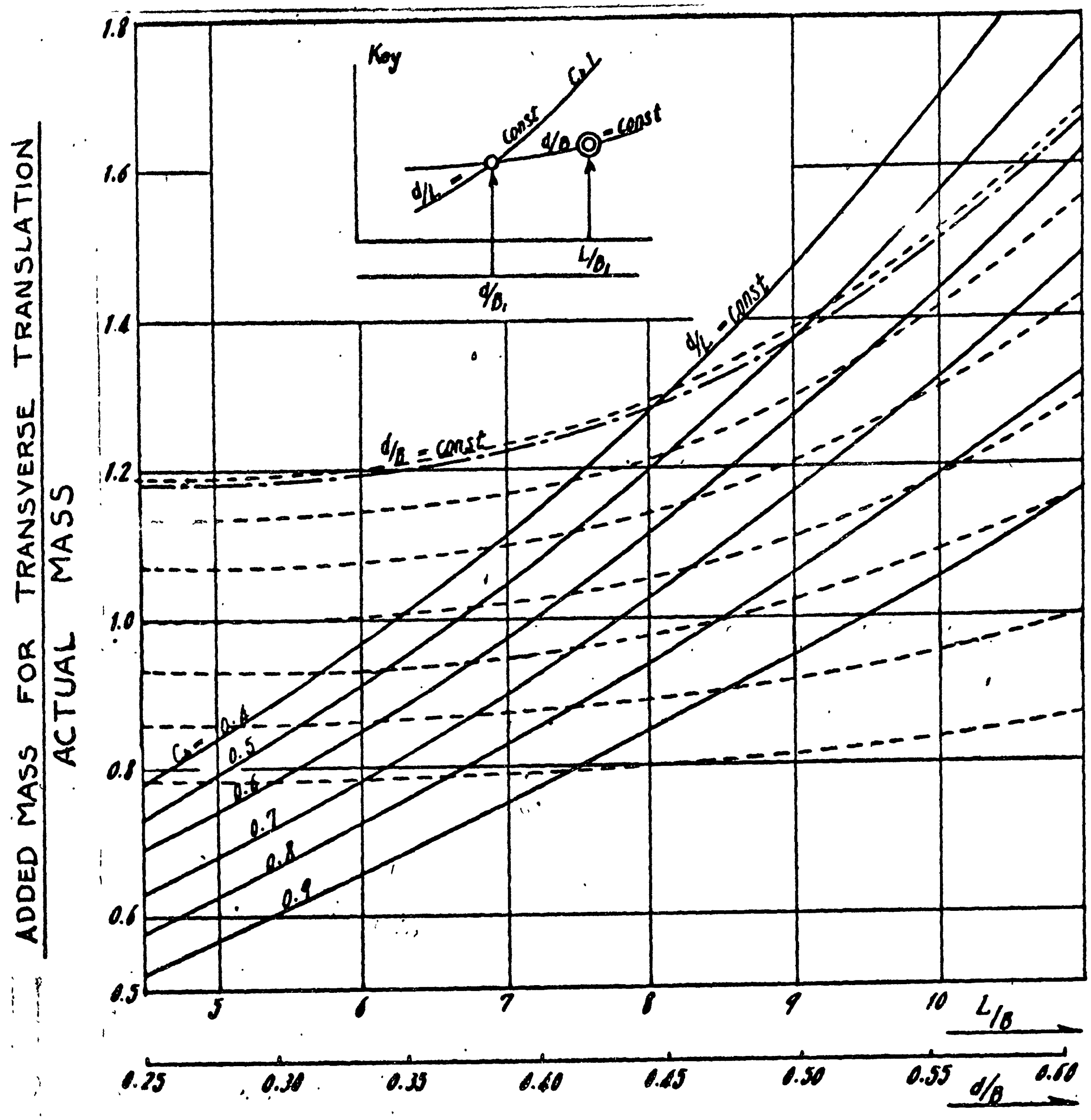

L Length

B Beam

d Draft

C_B Block coefficient

This figure is taken from the paper by Motora (1960)

FIGURE 7

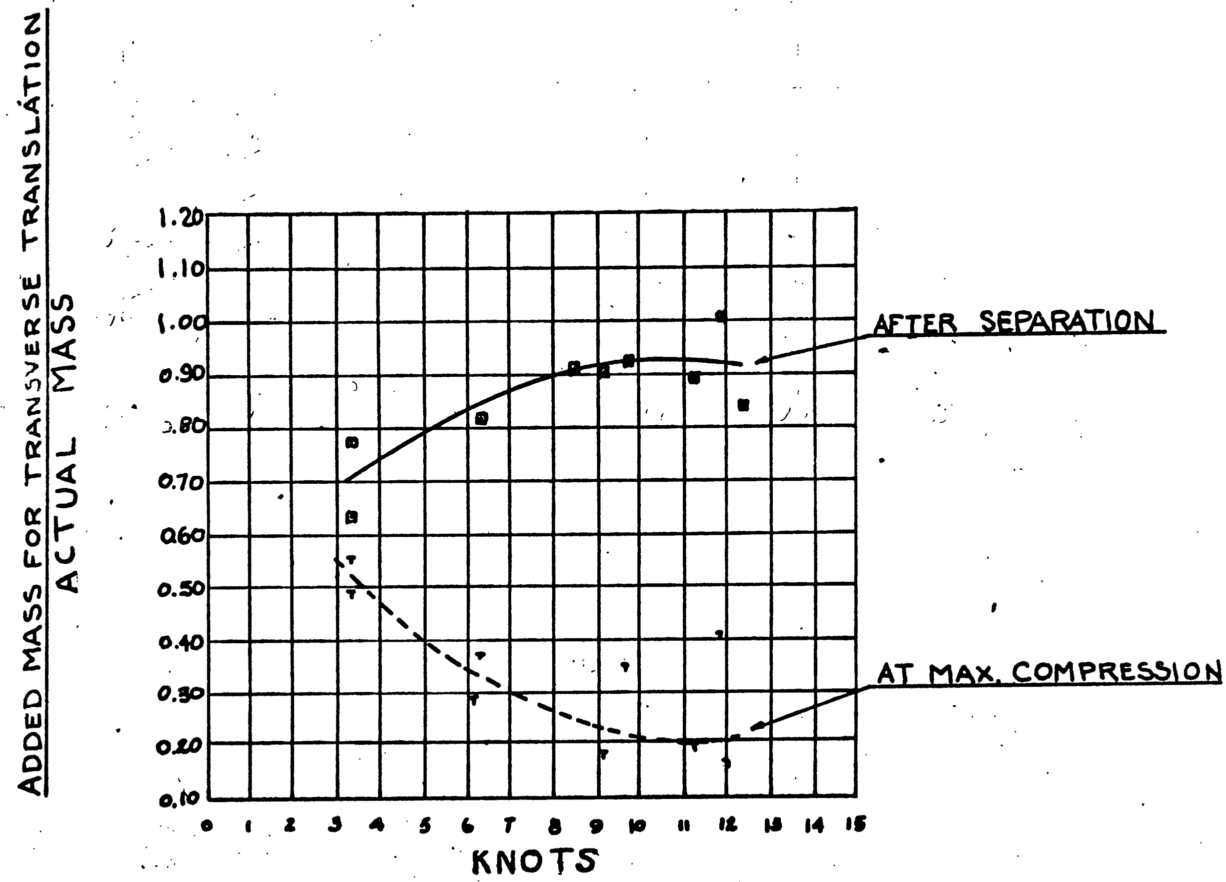

This figure is taken from Spinelli (1962)

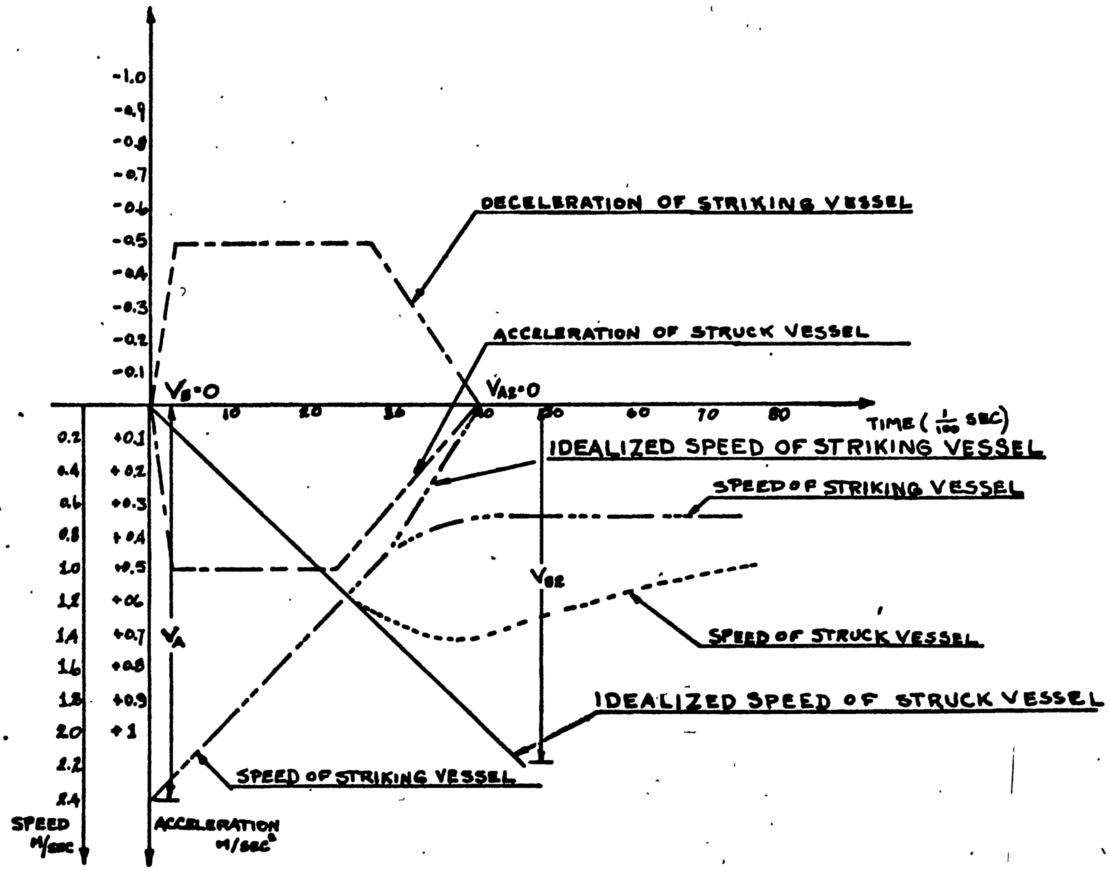

The acceleration and deceleration shown are idealized

Evalution by Spinelli: using idealized V_{B2} and V_{A2}:

$$e = - \frac{V_{A2} - V_{B2}}{V_A - V_B} = \frac{1.90}{2.42} = 0.785$$

This figure is taken from Spinelli (1964)
(Notation as used in this paper)

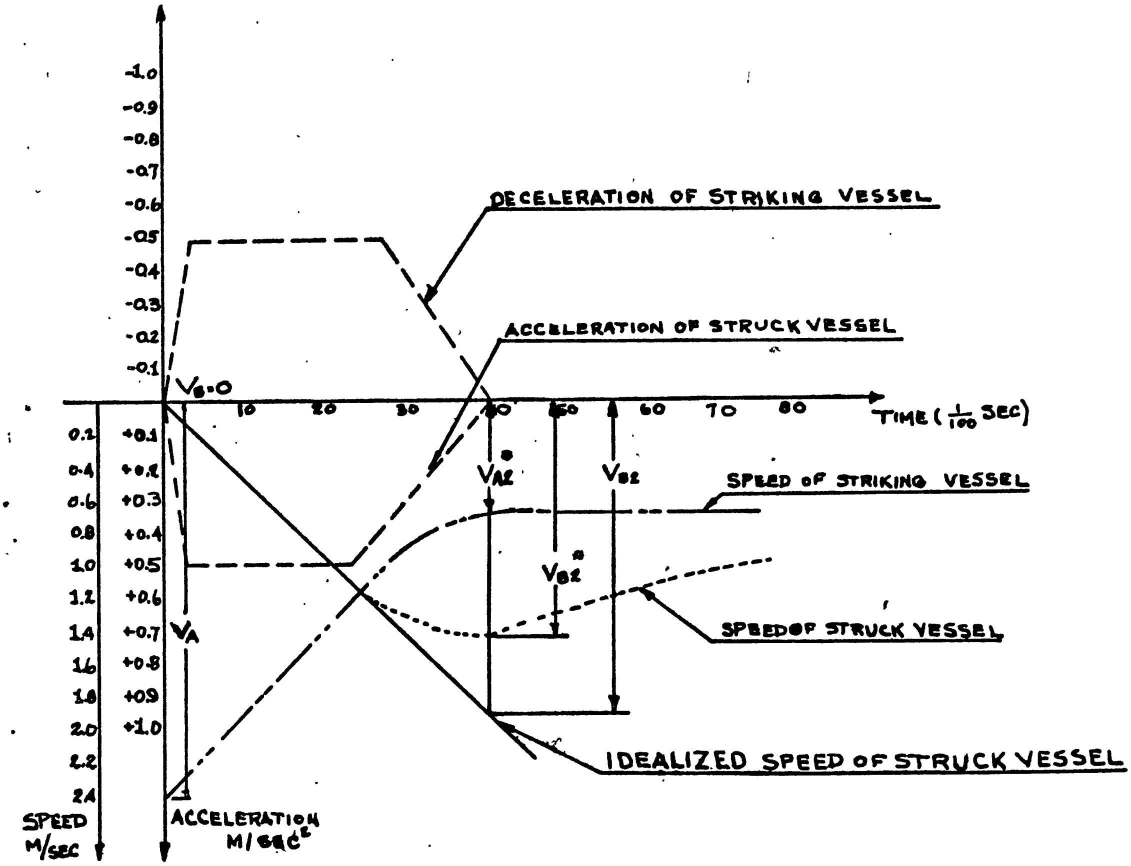

The acceleration and deceleration shown are idealized

Two possible evaluations different from that by Spinelli: using V_{B2} and $V_{A2}*$

$$e = -\frac{V_{A2}* - V_{B2}}{V_A - V_B} = \frac{1.90 - 0.75}{2.42} = 0.475$$

using $V_{B2}*$ and $V_{A2}*$

$$e = -\frac{V_{A2}* - V_{B2}*}{V_A - V_B} = \frac{1.45 - 0.75}{2.42} = 0.289$$

FIGURE 10

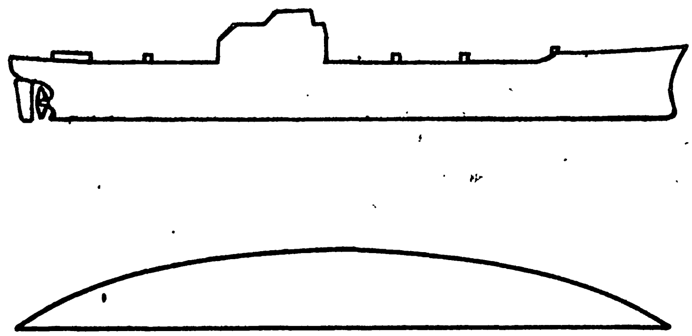

a) Longitudinal Mass Distribution

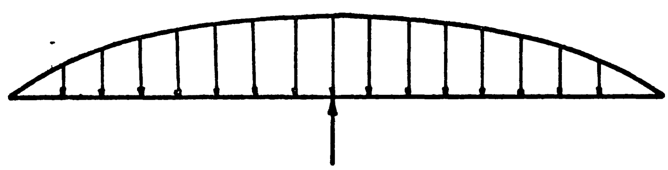

b) Inertia Forces and Impact Force
(including added mass effect)

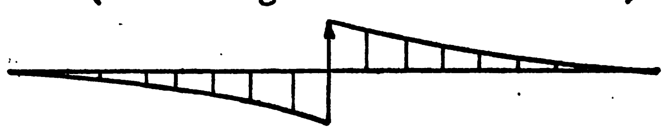

c) Shear Curve

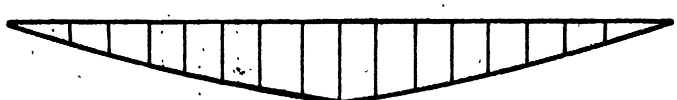

d) Bending Moment Curve

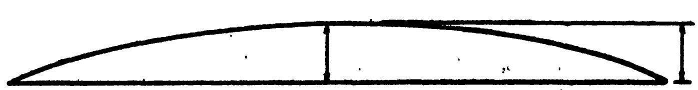

e) Deflection Curve

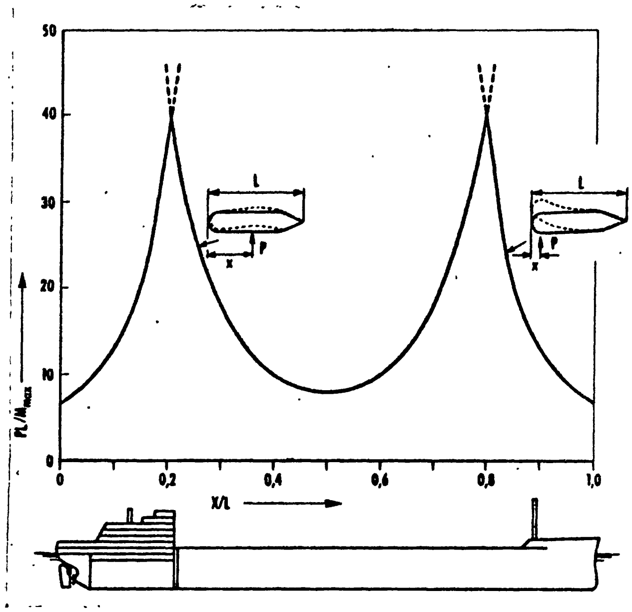

P	Impact Force
L	Ship Length
X	Location of Damage
M_{MAX}	Standard Bending Moment

This figure is taken from Woisin (1964a)

<u>FIGURE 12</u> - Experimental set-up used in Japan

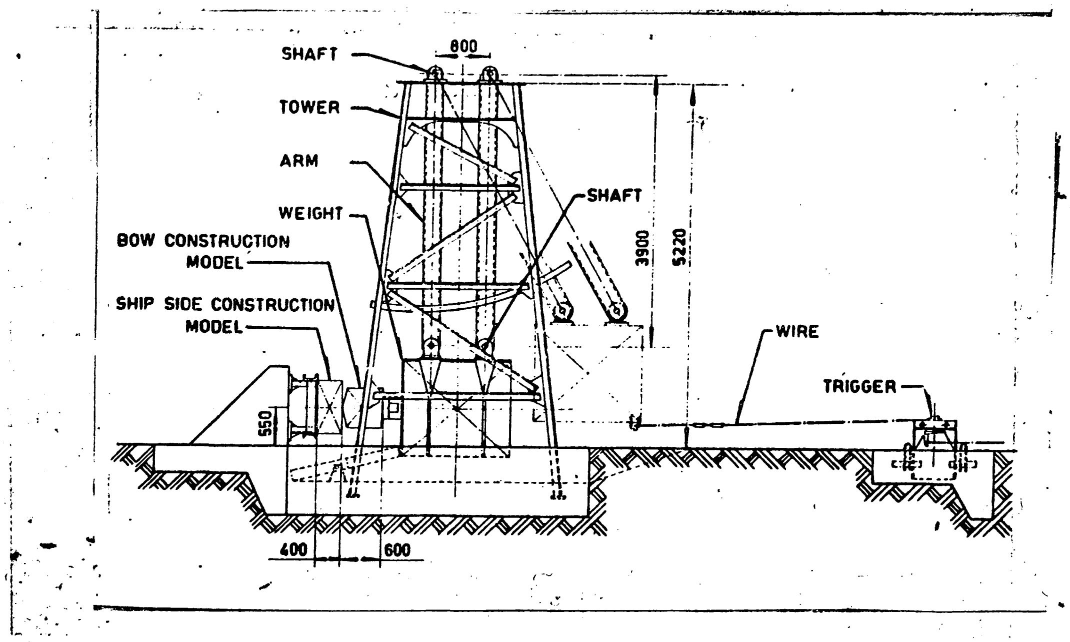

This figure is taken from Kagami (1960)

<u>FIGURE 13</u> - Experimental set-up used in Italy

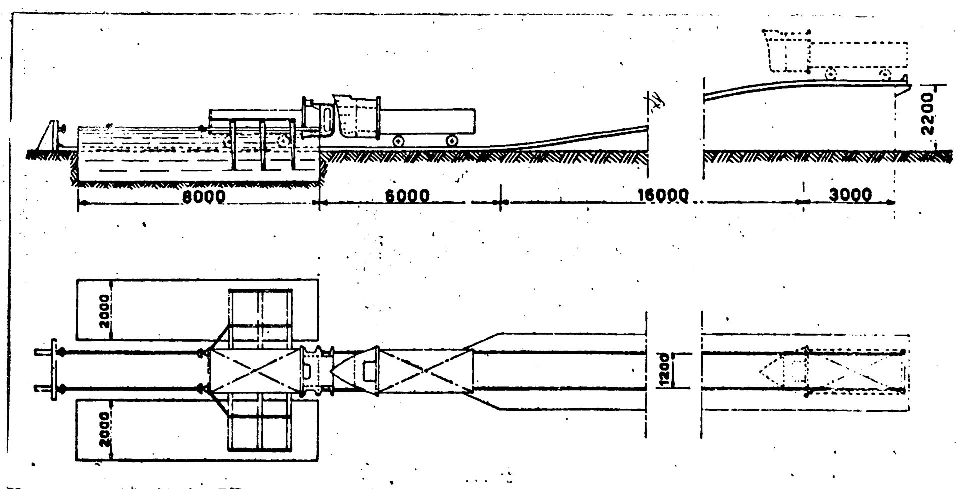

This figure is taken from Spinelli (1962)

FIGURE 14

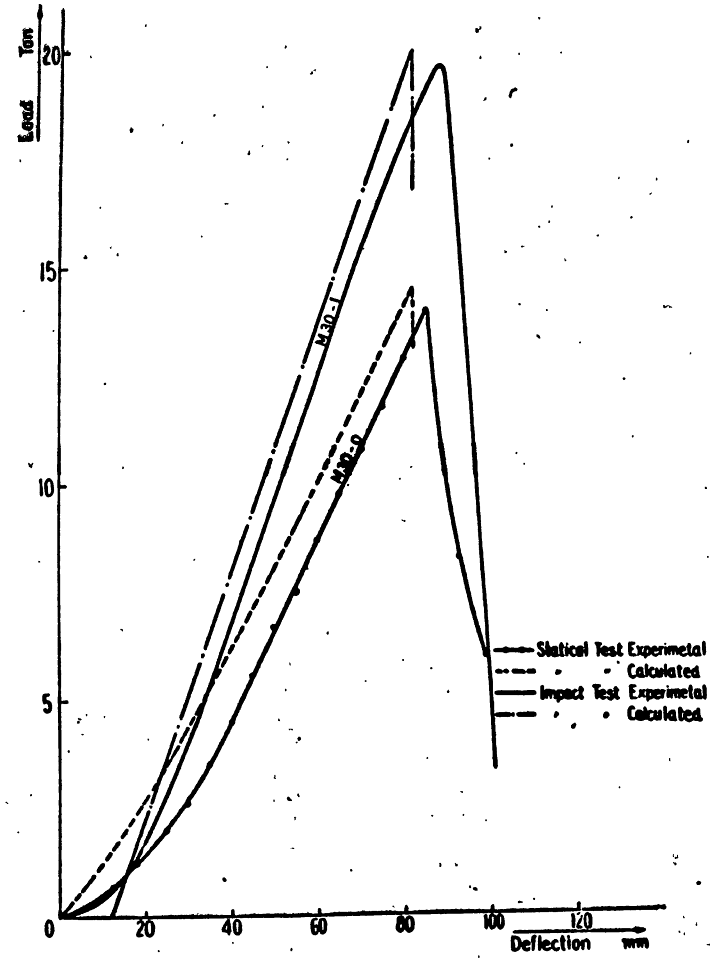

Load vs. Deflection for square plate

This figure is taken from (Study 1962)

FIGURE 15a- Impact Load Against Deflection

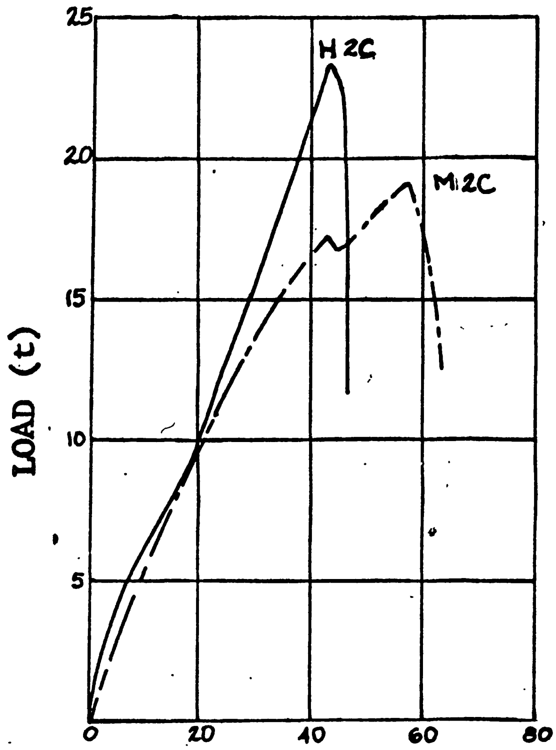

Deflection (mm)
Taken from (Study 1961)

FIGURE 15b- Impact Load Against Deflection

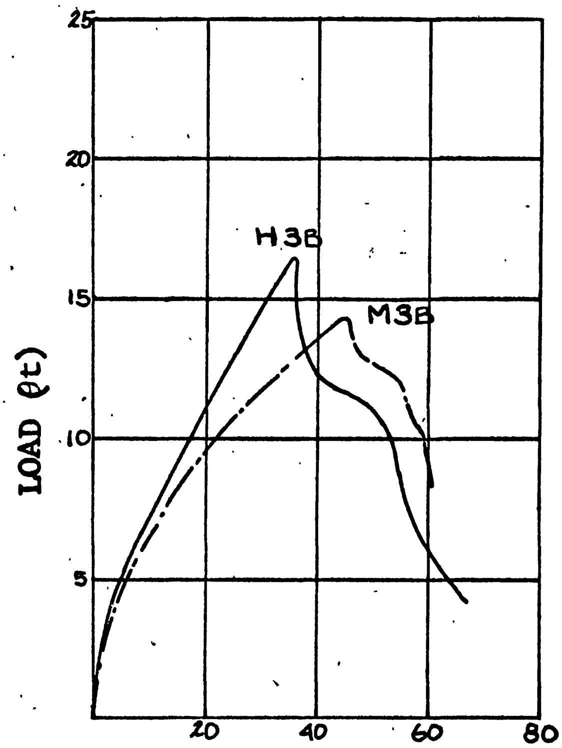

Deflection (mm)
Taken from (Study 1961)

FIGURE 15c- Impact Load AgainstDDeflection

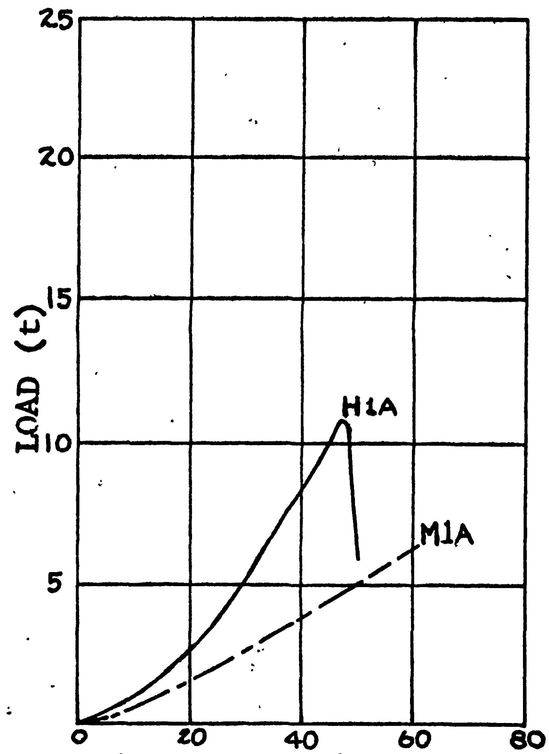

Deflection (mm)
Taken from (Study 1961)

FIGURE 15d - Impact Load Against Deflection

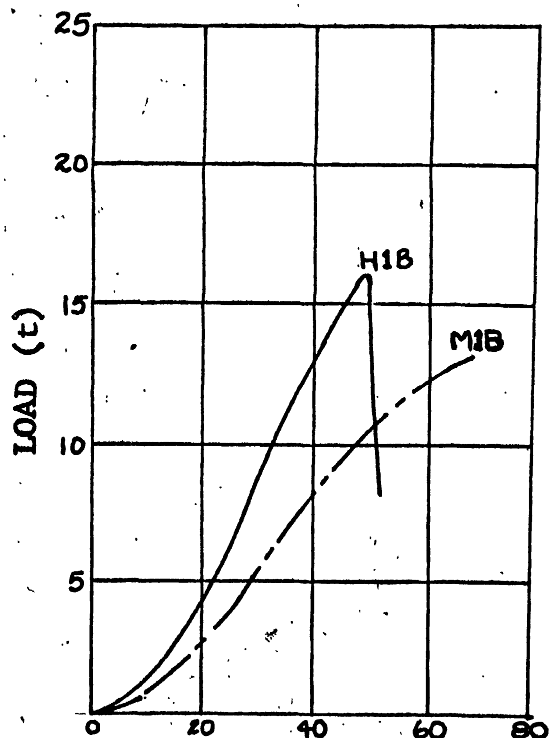

Deflection (mm)
Taken from (Study 1961)

FIGURE 16

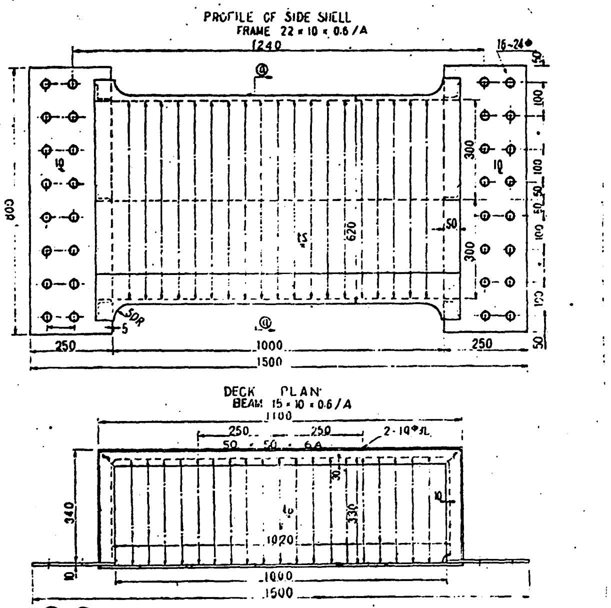

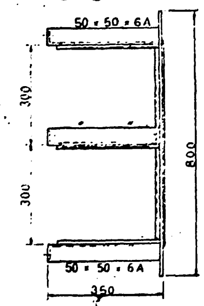

MARK	THICKNESS	
	SIDE (t_S)	DECK (t_D)
S1 - 1	23	07
S1 - 2	16	12
S1 - 3	10	16

Model of Side Structure - Type S-1

FIGURE 17

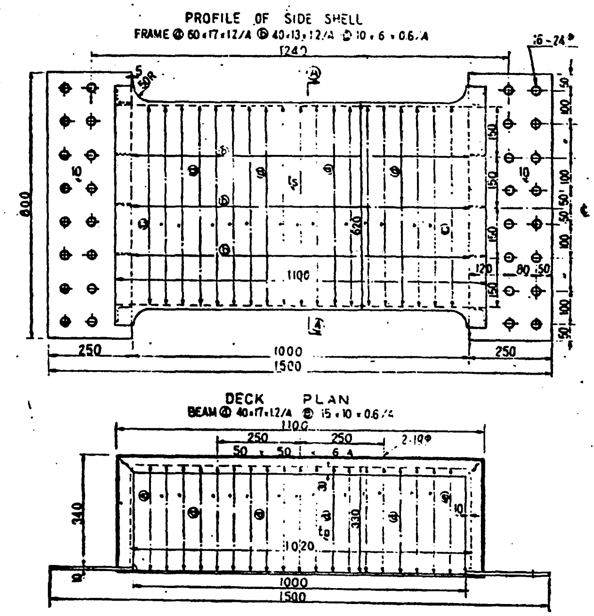

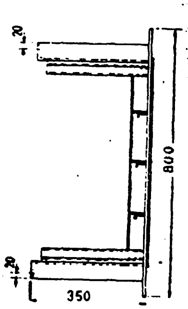

MARK	THICKNESS	
	SIDE (t_S)	DECK (t_D)
S2 - 1	23	06
S2 - 1	16	12

Model of Side Structure - Type S-2

These figures are taken from (Study 1963)

FIGURE 18

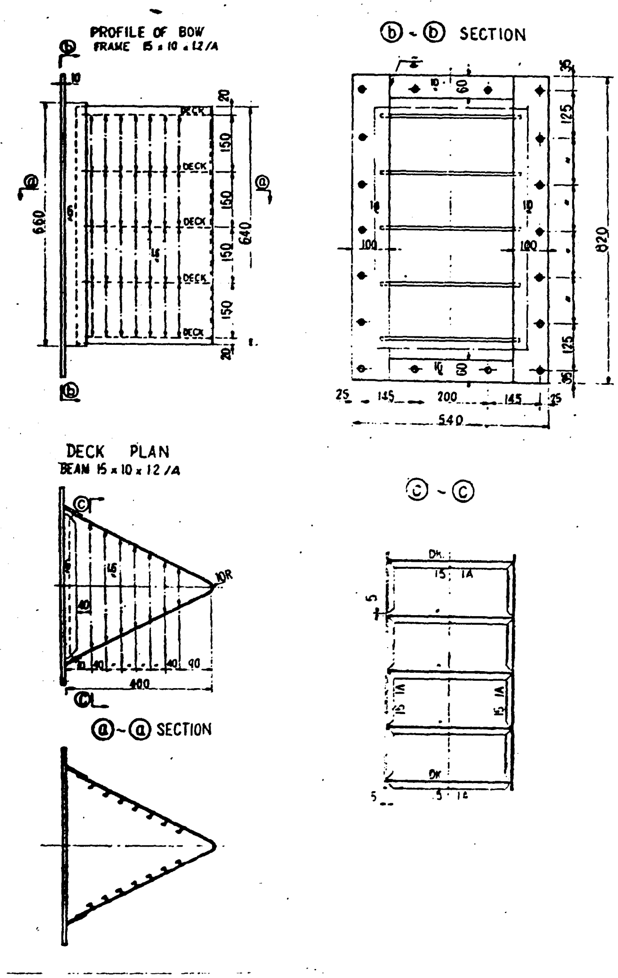

Bow Model - Type B-2

FIGURE 19

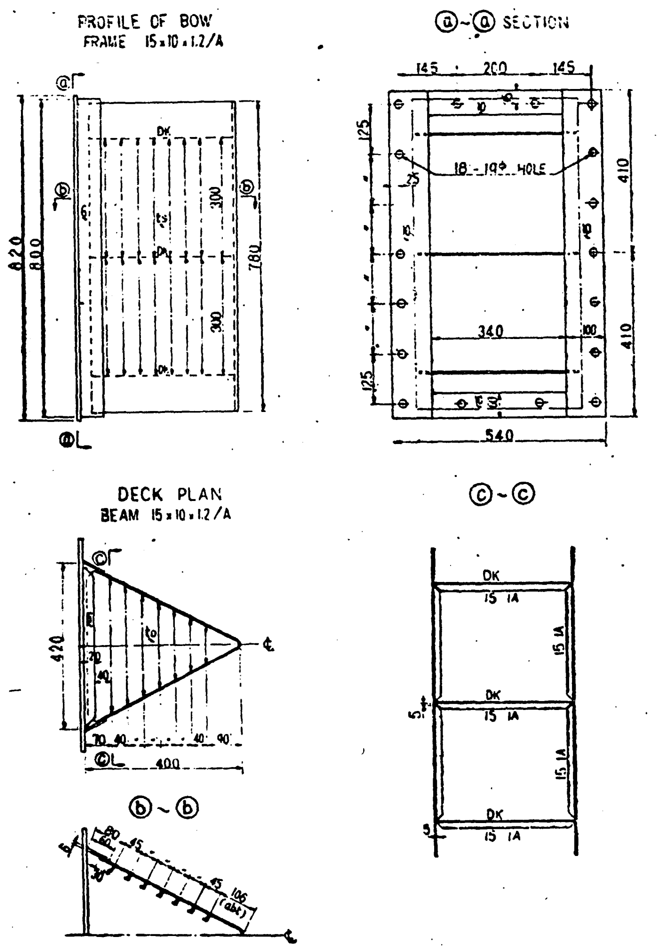

Bow Model - Type B-2

These figures are taken from (Study 1963)

FIGURE 20

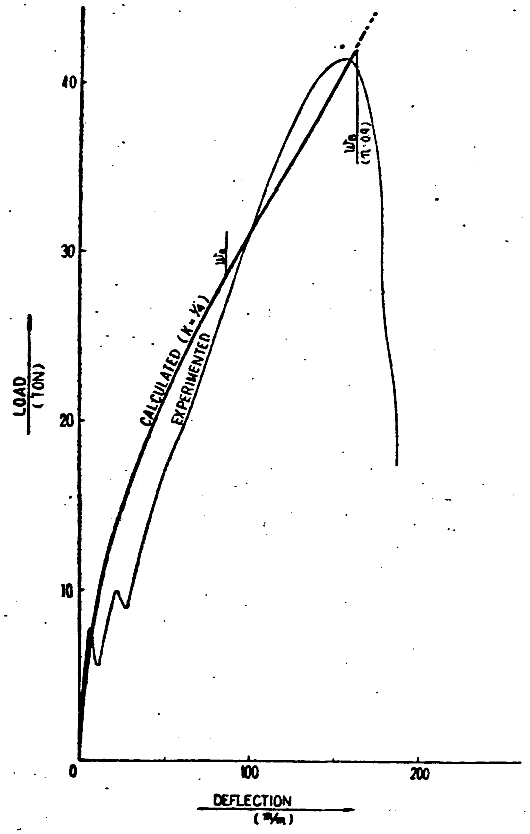

Load-Deflection Curve

S 1-1 Impact Test

FIGURE 21

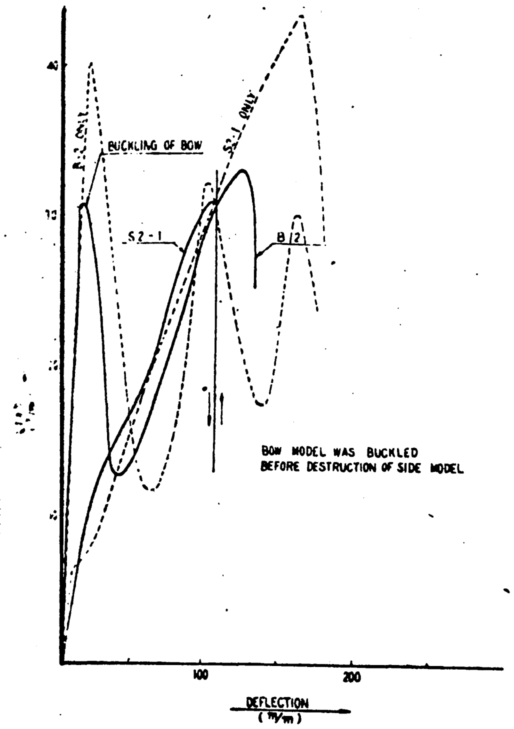

FIGURE 22

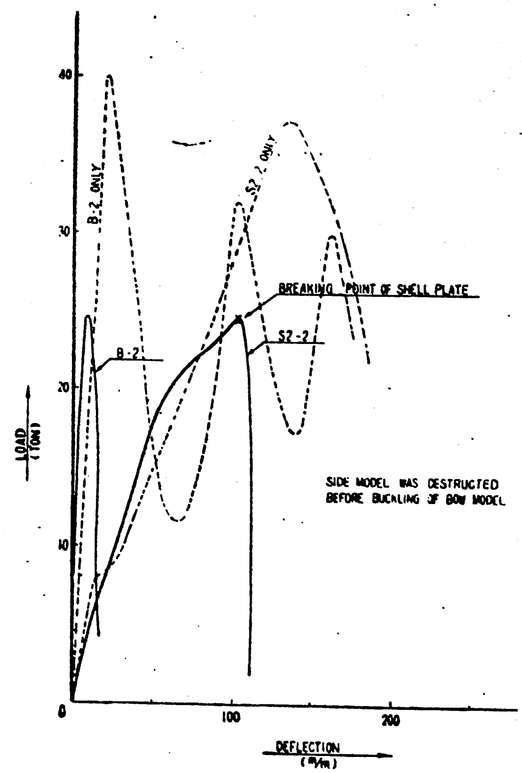

Load-Deflection Curves

B-2/S 2-1 Impact Test

B-2/S 2-2 Impact Test

These figures are taken from (Study 1963)

FIGURE 23

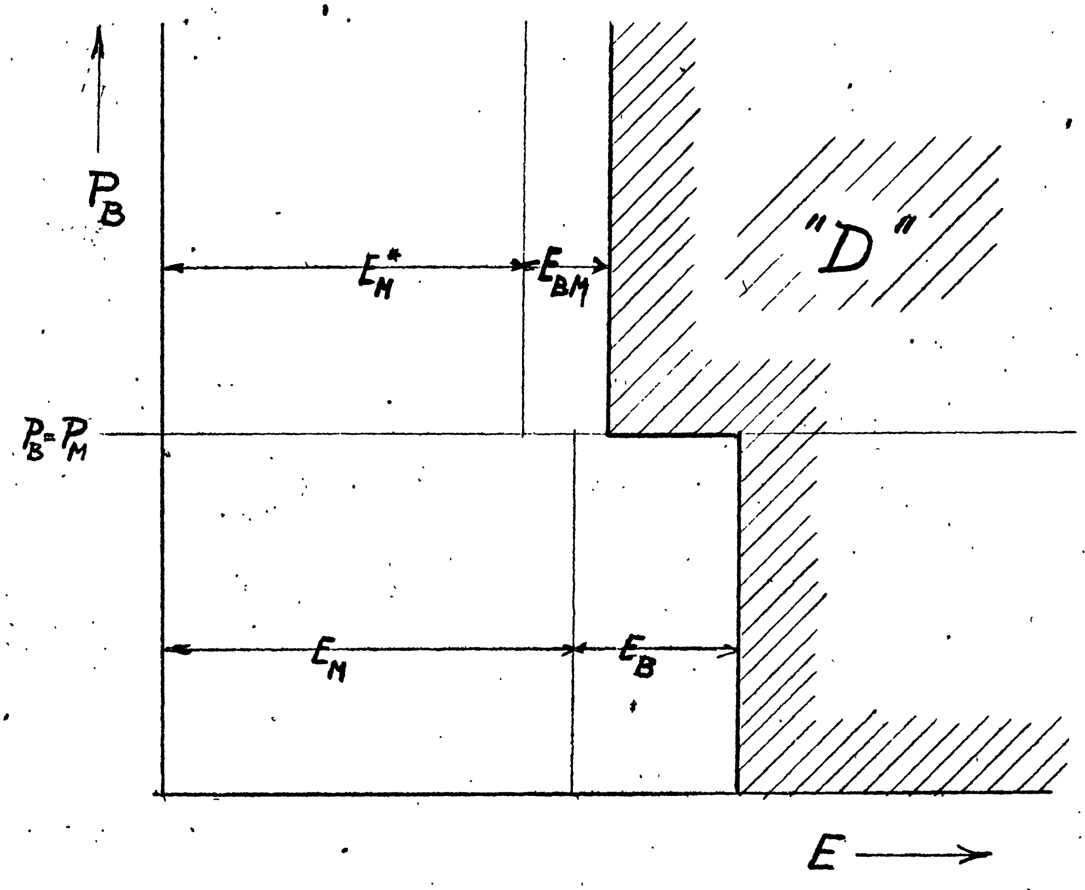

FIGURE 24: Log-Normal Distribution (truncated)

Distribution Density

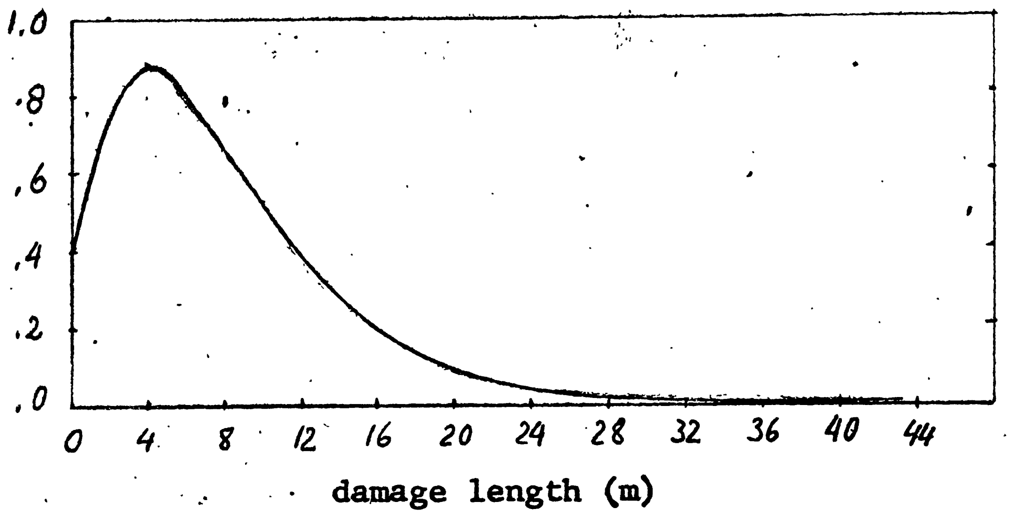

Distribution Function

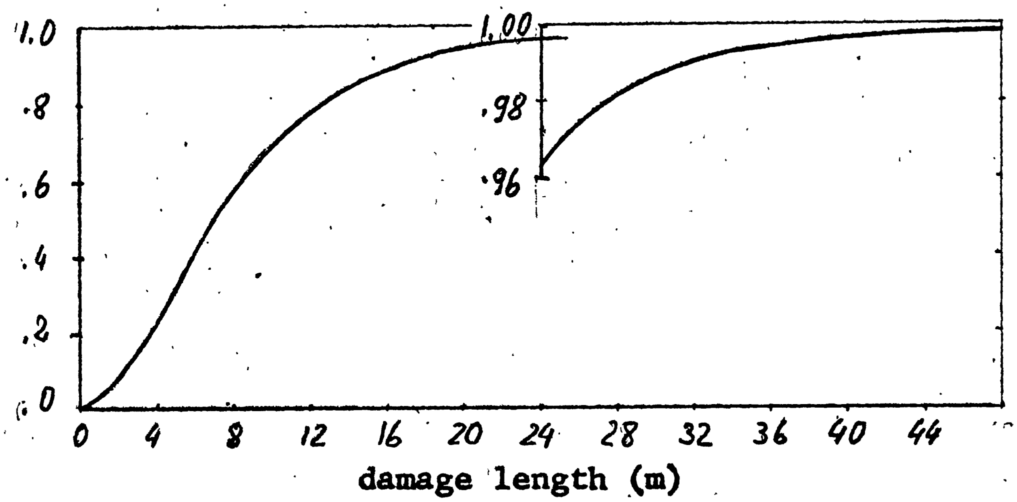

FIGURE 25

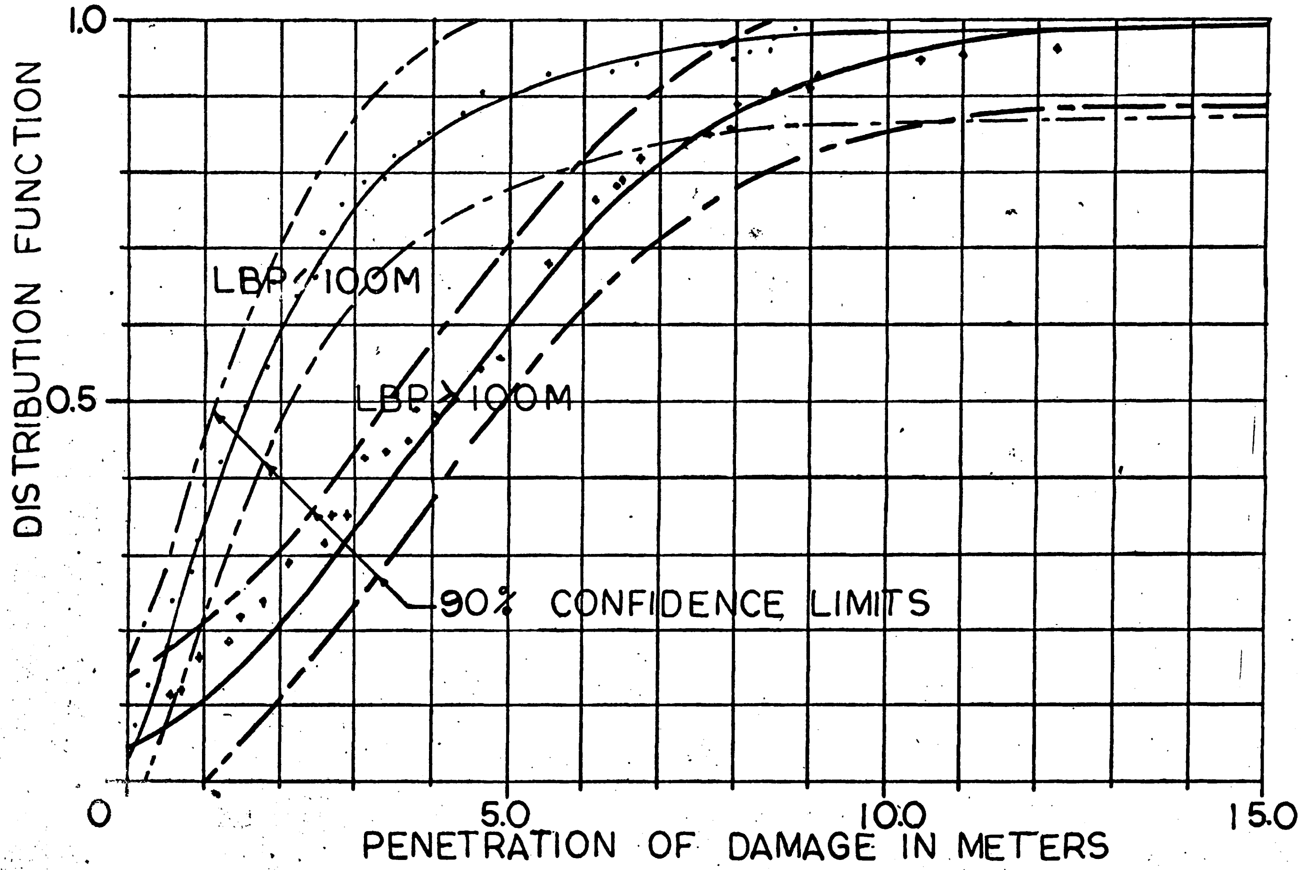

Length	LBP < 100 M	LBP > 100 M
Ships	104	141
90% Confidence Limits	11.95%	10.3%
Mean	2.2 M	4.6 M
Standard Deviation	2.2 M	4.9 M
Median	1.6 M	4.3 M
Upper Decile	4.9 M	8.5 M
Lower Decile	0.2 M	1.0 M

FIGURE 26 - Frequency of Location of Damage

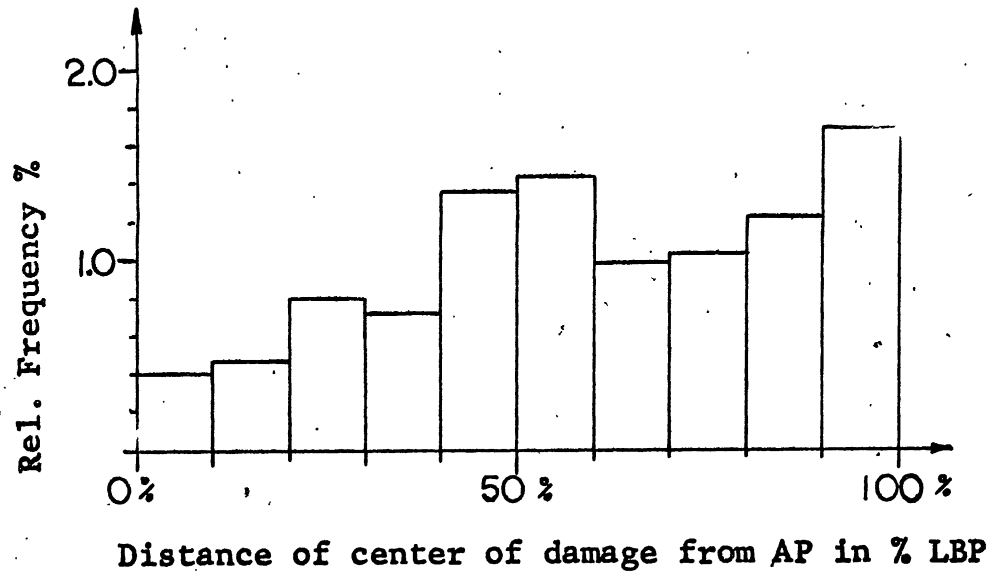

FIGURE 27 - Median of Damage Length Vs. Location of Damage

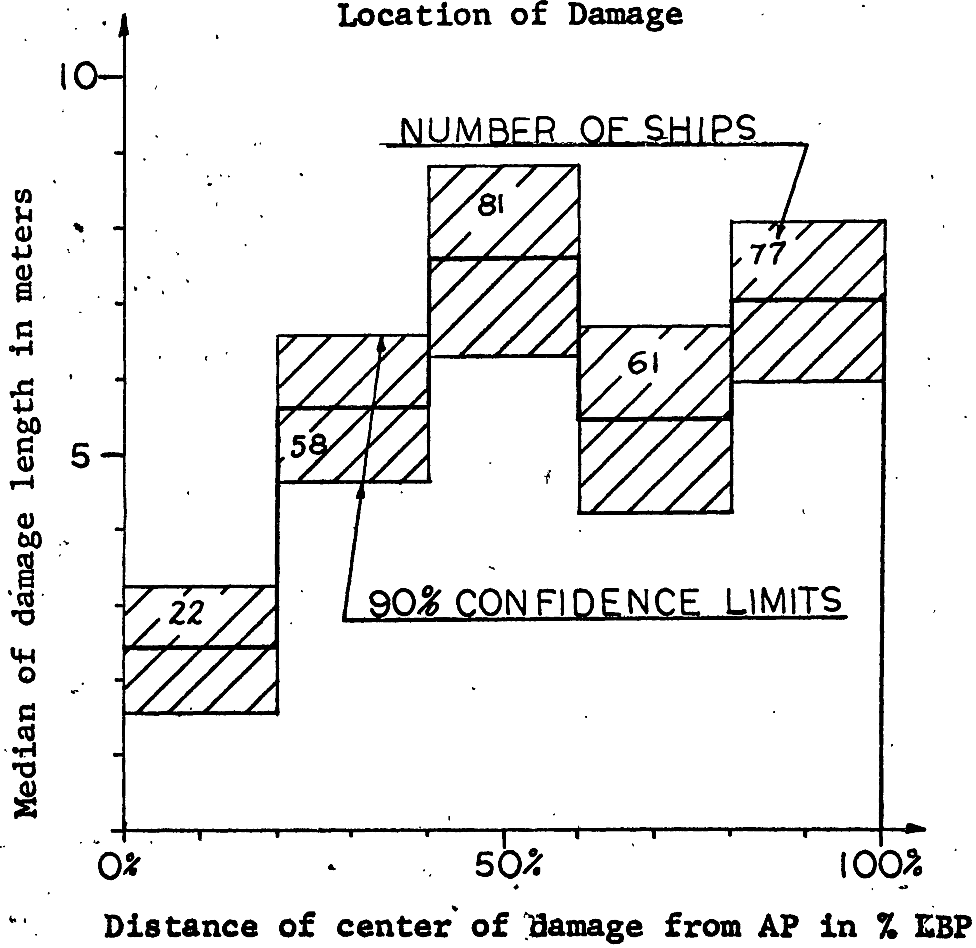

FIGURE 28

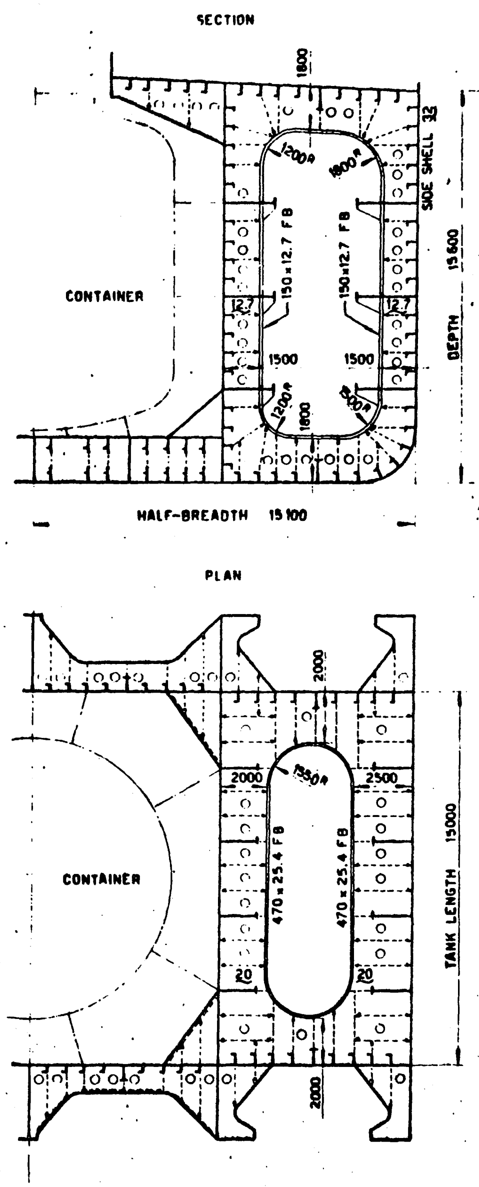

28

FIGURE 29

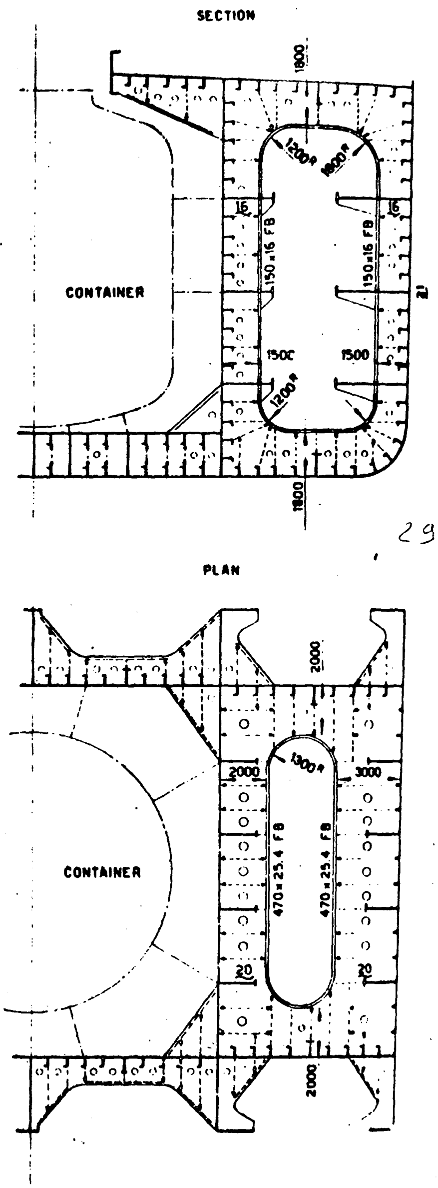

29

These figures are taken from Kagami (1960)

FIGURE 30

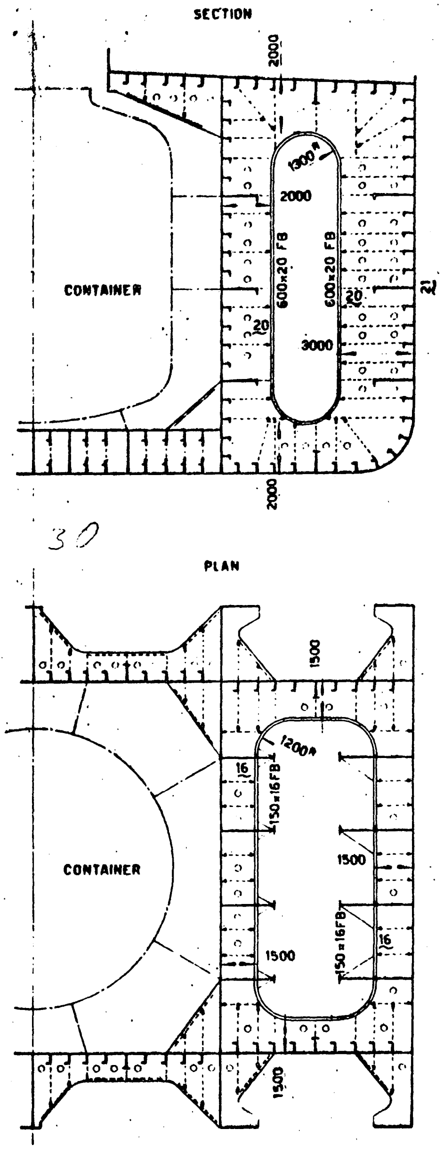

FIGURE 31

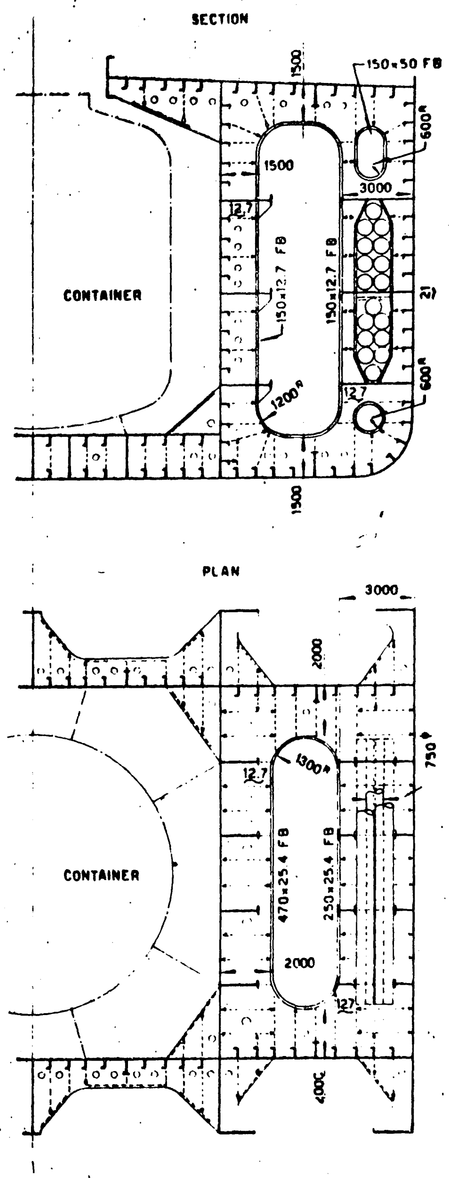

These figures are taken from Kagami I (1960)

FIGURE 32

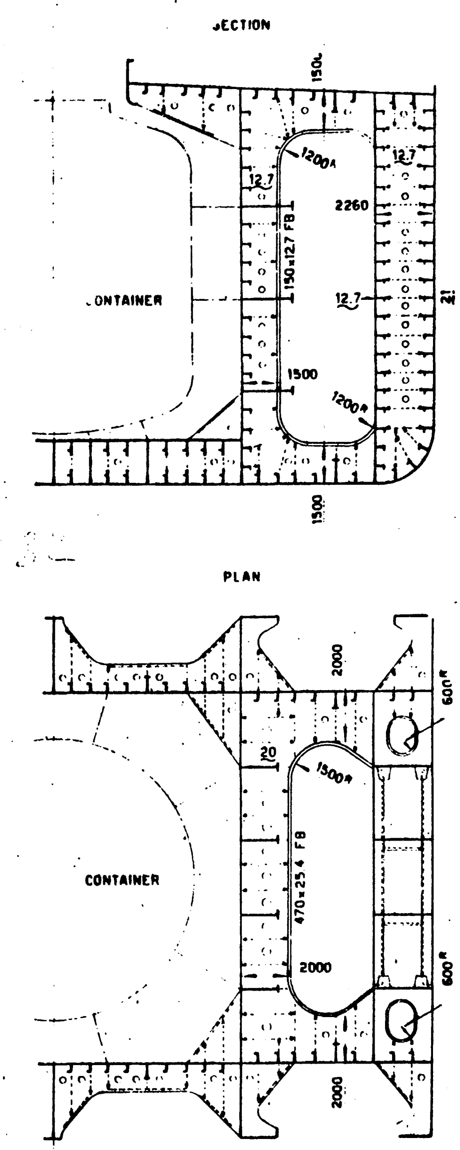

FIGURE 33

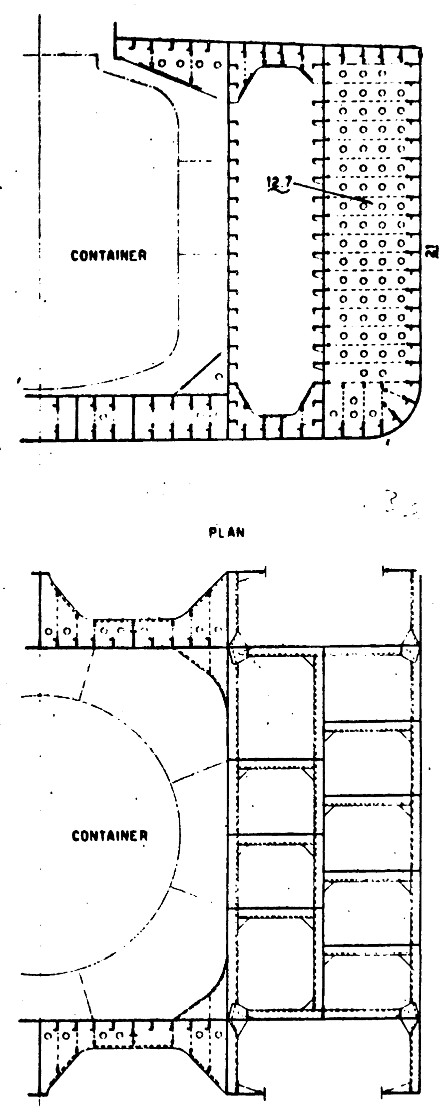

These figures are taken from Kagami (1960)

FIGURE 34

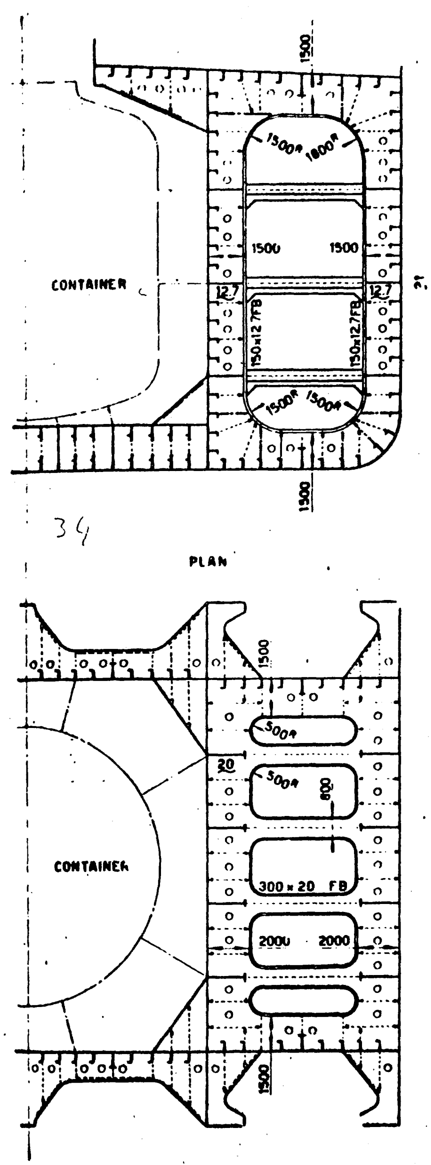

FIGURE 35

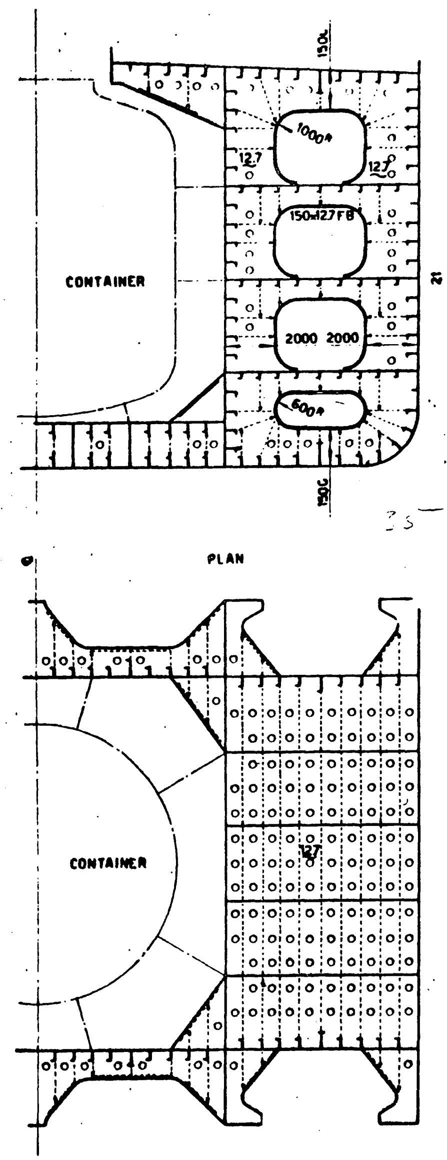

These figures are taken from Kagami (1960)

FIGURE 36

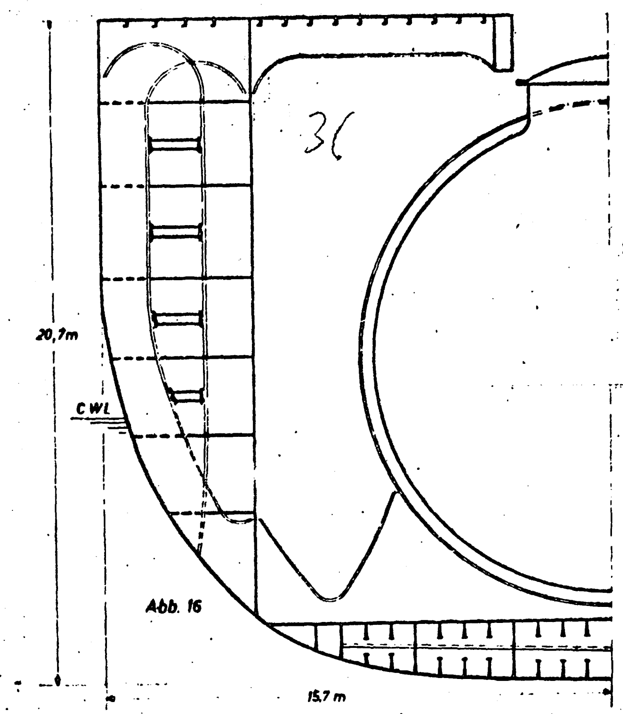

FIGURE 37

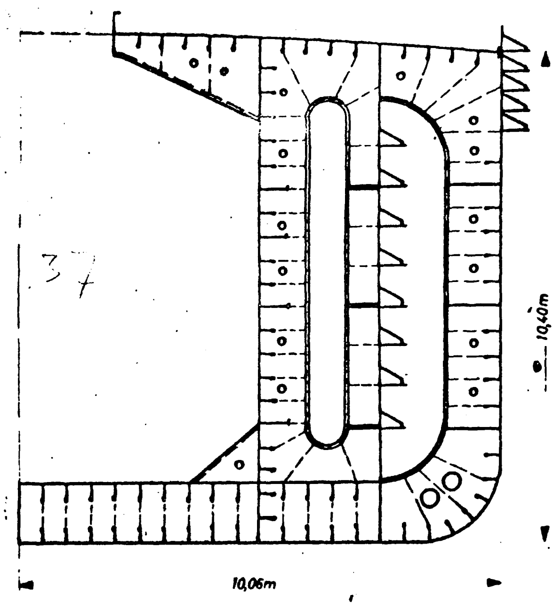

FIGURE 38

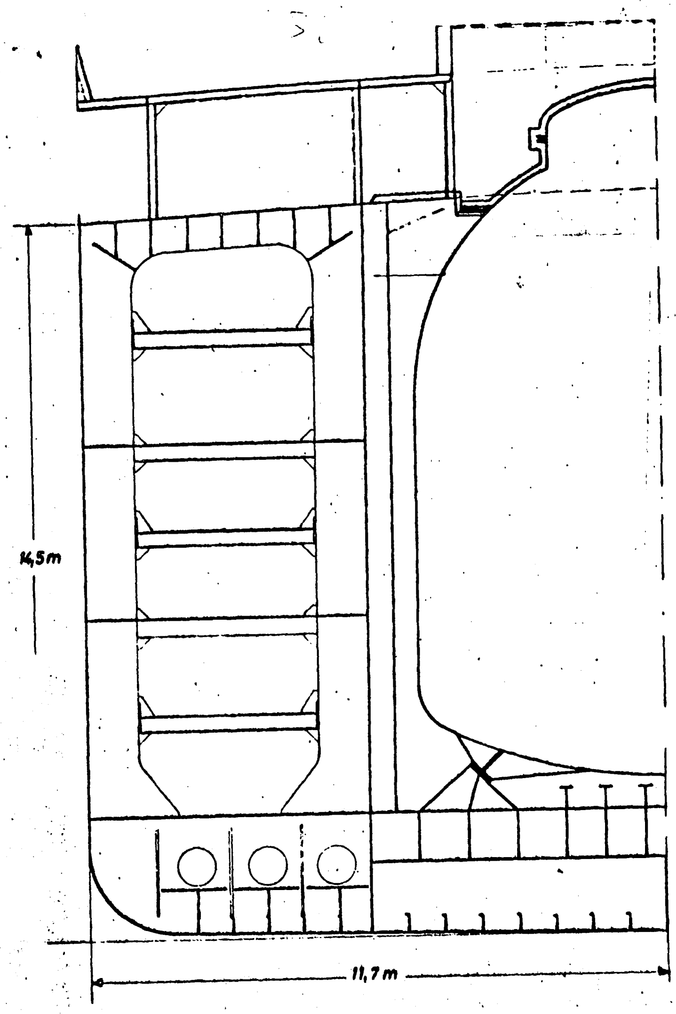

Figures 36 and 38 are taken from Woisin (1964a).

Figure 37 is taken from Spinelli (1961)